 doi:10.20944/preprints202102.0380.v1

Green Synthesis of Transition Metals Nanoparticle and their Oxides: A Review

Sean Drummer, Tafirenyika Madzimbamuto & Mahabubur Chowdhury*

Department of Chemical Engineering, Cape Peninsula University of Technology, Symphony way, Bellville, 7535

*Corresponding author: chowdhurym@cput.ac.za

Abstract

In recent years, many researchers have begun to shift their focus onto the synthesis of nanomaterials as this field possesses immense potential that may provide incredible technological advances in the near future. The downside of conventional synthesis techniques, such as co-precipitation, sol-gel and hydrothermal methods, is that they necessitate the use of toxic chemicals, produce harmful by-products and require a considerable amount of energy; therefore, more sustainable fabrication routes are sought after. Biological molecules have been previously utilised as precursors to nanoparticle synthesis, thus eliminating the negative factors involved in traditional methods. In addition, transition-metal nanoparticles possess a wide scope of applications due to their multiple oxidation states and large surface areas; thereby allowing for a higher reactivity when compared to their bulk counterpart and rendering them an interesting research topic. However, this field is still relatively unknown and unpredictable. Therefore, this review aims to obtain a better understanding on the plant-mediated synthesis process of the major transition-metal and transition-metal oxide nanoparticles, and how different parameters affect their unique properties.

Keywords

Nanoparticle; transition-metal; transition-metal oxides; plants; green synthesis; factors*

Preprints (www.preprints.org) | NOT PEER-REVIEWED | Posted: 17 February 2021 doi:10.20944/preprints202102.0380.v1

1. Introduction

Due to recent advancements and developments in industry, the environment has suffered tremendously, with toxic wastes regularly being released into the ecosystems, causing irreparable damage to biological life and infrastructures. Therefore, it is necessary for all engineering and technological aspects to move to a more sustainable area. One of the most rapidly developing industries is the “nano industry,” where nanotechnology could possibly bring about a new industrial revolution.

Nanotechnology refers to the field of applied science and technology which involves the manipulation of matter on a molecular and atomic scale with several prospective applications [1]. Nanoparticles are defined as certain complexes of solid units that possess sizes between 1 and 100 nm. The most unusual aspect of nanoparticles is that they retain a large surface area due to the minute size of the particles when compared to their bulk counterpart. This characteristic of the nanomaterial allows for higher reactivity and denotes specialised properties to them [2]. Due to these attributes, nanoparticles are applied in chemical, biological and industrial fields.

Transition metals are defined as *d*-block elements as their atomic structures have incomplete *d*-orbitals in their electron configuration and, therefore, give rise to physical and chemical properties that differ from the main group elements [3]. These elements are considered interesting for research as they retain multiple oxidation states caused by the proximity in energy of the *d* and *ns* shells [4]. This provides a large number of configurations for their oxides, thus, widening the field of applications for transition metals. Despite this, literature lacks a state-of-the-art review on the application of these compounds.

Certain physical and chemical processes have been established for the synthesis of metal nanoparticles and their oxides. Through copious research and experimentation, these methods have become well-defined, where the physiochemical properties of the nanostructures can be excellently controlled and tailored as needed. The conventional techniques have been listed under top-down and bottom-up methods in Figure 1, However, these procedures have several disadvantages as they require the use of toxic chemicals, produce harmful by-products and necessitate high energy consumptions (Singh et al, 2018). Hence, it is essential for the further development of the environmentally friendly approach to synthesise metal and metal oxide nanomaterials.

Preprints (www.preprints.org) | NOT PEER-REVIEWED | Posted: 17 February 2021 doi:10.20944/preprints202102.0380.v1

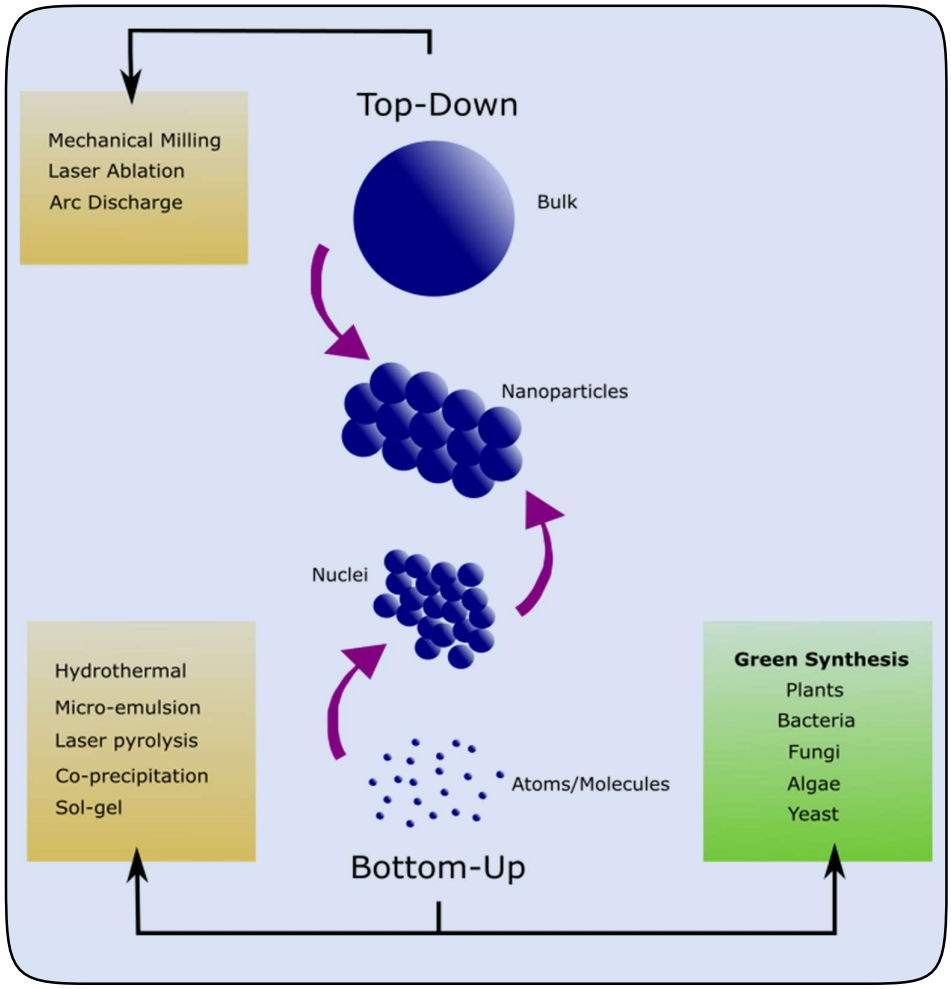

Figure 1: Various Approaches for the Synthesis of Nanoparticles

Through previous studies, it has been established that various biological routes may be utilised for the fabrication of nanoparticles through the use of plants [5], bacteria [6], fungi [7], algae [8] and yeast [9] as they contain metabolites that possess the ability to reduce metallic salts and formulate nanoparticles. In addition, these substances do not only act as a reducing agent, they are also involved in the stabilisation of the nanostructures. Since this area of "green" nanotechnology is relatively new [10], the problem lies with controlling the size and morphology of the nanoparticles due to the different characteristics and compositions of the biological mediums utilised during synthesis. This being said, the main objective is to achieve a better understanding on the green synthesis in order to acquire the desired size, shape, composition and dispersity, with an exceptional degree of repeatability if conventional approaches are to be replaced.

Therefore, this review will focus on summarising the current progress in plant-mediated synthesis of various transition-metal nanoparticles such as titanium, iron, cobalt, nickel, copper, zinc, palladium, silver, platinum, gold and their oxides. In addition, the advantages over the conventional synthesis techniques, green synthesis reaction mechanism, possible compounds responsible for the reduction reaction and critical process parameters are discussed. Ultimately, the objective is to present the procedures and results of green synthesised transition-metal/metal oxide nanoparticles for the enhancement of the literature in this field which may aid researchers in their future endeavours.

Preprints (www.preprints.org) | NOT PEER-REVIEWED | Posted: 17 February 2021 doi:10.20944/preprints202102.0380.v1

2. Biological Synthesis Techniques

Within the past three decades, solutions to the disadvantages of conventional nanoparticle techniques, such as the toxic reactants required, hazardous by-products produced and high energy consumption, have been sought. The main goal was to reduce the negative aspects of the aforementioned chemical methods (Figure 1) and create more sustainable methods to minimise pollution at the source instead of necessitating waste management procedures. Interestingly, nature provided the tools for a new, revolutionary technique that utilises plants and microorganisms for nanoparticle fabrication.

It was discovered that most autotrophs, that is, organisms that produce their own nutritional compounds using organic material in their vicinity, such as plants, fungi, bacteria and yeast possess a certain reducing capability which enables the material to react with metallic ions and form any desired nanoparticle [11–14]. The “green” synthesis of nanoparticles has some advantages over the conventional methods as they limit the use and production of toxic, inorganic chemicals and can be carried out in ambient conditions while still preserving the quality of the nanostructures with a relatively fast production rate [15]..

The procedure involves metal ions that undergo either oxidation or reduction, depending on the biological media utilised. The exact mechanisms for the biological synthesis of nanoparticles have not yet been extensively studied as each autotroph contains different compounds responsible for the reaction. However, it is known that the process is initiated through the nucleation of the metallic substance and, thereafter, nanoparticle growth commences where it is formed as the precipitate within the mixture (Figure 2). Furthermore, the organic material found in plants and microorganisms are also involved in the stabilisation, in other words capping, of the nanoparticles as they bind to the surface of the nanostructures, thereby preventing aggregation and negating the need for additional stabilising agents [16]

Preprints (www.preprints.org) | NOT PEER-REVIEWED | Posted: 17 February 2021 doi:10.20944/preprints202102.0380.v1

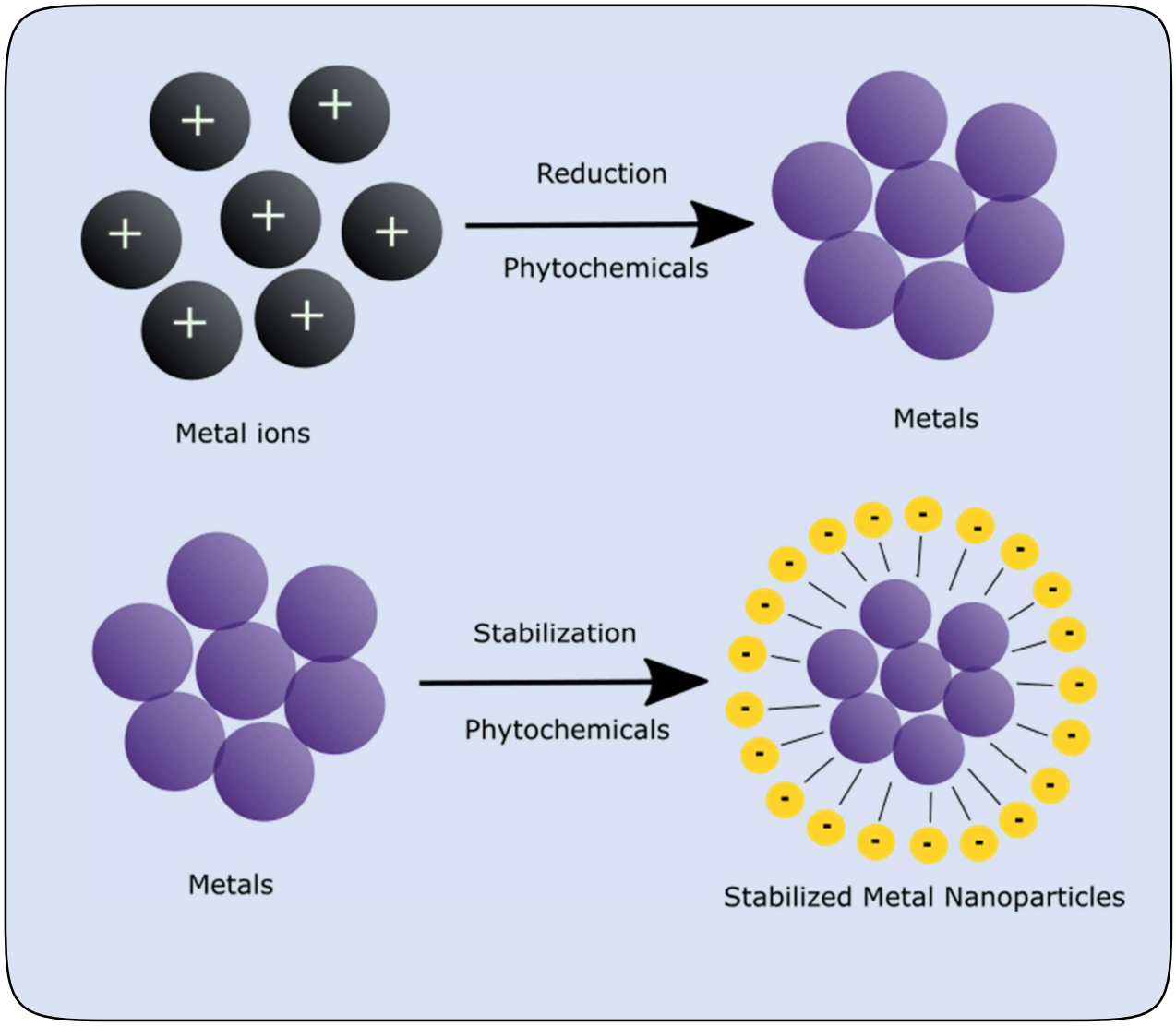

Figure 2: The Growth Mechanism of Nanoparticles through the use of Plant Extracts

According to research, in order to reproduce this process in a laboratory environment, plant extracts seem to be the superior biological mediums as they are more stable, reduce metal ions at a faster rate and easier to scale-up than microorganisms [16–18]. Therefore, plants have been the main focus of research into the biosynthesis of nanoparticles as they also retain a high synthesis success rate when compared to microorganisms [19].

Previous research has shown that the primary and secondary metabolites of plants are responsible for the reduction of metallic ions during the synthesis procedure [20]. These major phytochemicals are categorised within the supplementary document from Table S1 to S5. They include terpenoids, phenols, carbohydrates, saponins, alkaloids and proteins. These compounds are expected to induce some shape control during the reduction reaction [21]. Hence, the variation in composition and concentration of the active biomolecules between plant species and their behaviour with the metallic reactants is believed to be the main contributing factors to the diverse aspects of the nanomaterial, and the screening of phytochemicals with higher electron donating capacities may positively impact future research in the plant-based synthesis of nanoparticles [19,22]. This being said, the optical and electrical properties of the nanoparticles are highly dependent on the size and morphology and it is

Preprints (www.preprints.org) | NOT PEER-REVIEWED | Posted: 17 February 2021 doi:10.20944/preprints202102.0380.v1

important to achieve full control of these characteristics for further development in the field of "green" nanotechnology.

3. Green Synthesis of Transitional Metals & their Oxides

The synthesis of nanoparticles using the aqueous extracts of plant materials is a simple procedure that merely involves the use of plant extract as a reducing agent, with the mixture of a metallic salt solution. Transition-metal nanoparticles have been the prime focus of researchers due to the vast and interesting applications they possess. Section 3 focuses on the green synthesis of titanium-, iron-, cobalt-, nickel-, copper-, zinc-, palladium-, silver-, platinum- and gold-based nanoparticles, from 2005 to date, which include various process parameters with their resulting particle sizes and morphologies. This was accomplished through the analysation of published litertaure that involve various plant extracts for the synthesis of transition-metal and transition-metal oxide nanoparticles.

3.1. Titanium and Titanium Dioxide

The biosynthesis of pure titanium nanoparticles is extremely rare, however, one of the only attempts to synthesise the nanostructures was executed through the use of *Azadirachta indica* in a study conducted by Krishnasamy et al. (2015). After characterisation, the nanomaterial was found to be crystalline in nature with a mixture of rutile and anatase phases. In addition, the nanostructures possessed spherical morphologies with a size range of 15-42 nm.

Kalyanasundaram & Prakash (2015) demonstrated the green synthesis of titanium dioxide nanoparticles using *Pithecellobium dulce* and *Lagenaria siceraria* aqueous leaf extracts from titanium tetra-isopropoxide ($Ti(OCH(CH_3)_2)_4$) as a precursor. Their study compared the biologically synthesised nanocrystals to those of the chemical synthesis methods, where the sol-gel technique was adopted as the chemical synthesis route. The nanoparticles synthesised were predominantly spherical, with the *Pithecellobium dulce* synthesis obtaining the smallest particle size of approximately 6.3 nm and the chemically synthesised titanium dioxide possessing the largest diameter of 14.4 nm. Furthermore, a study conducted by Dobrucka (2017) resulted in the successful synthesis of titanium dioxide nanoparticles with the use of aqueous *Arnicae anthodium* extract as a bioreducing and capping agent [25]. The XRD study conducted on the nanopowder confirmed the average particle size to be approximately 30 nm.

Previous studies that focused on the plant-mediated synthesis of titanium dioxide nanoparticles (Table S6) produced mainly spherical particles that possessed a particle size range of approximately 40 nm; however, there were occasions where uncommon morphologies were experienced, such as tetragonal, oval, rod and triangular shapes which were synthesised through the use of *Citrus sinensis*, *Vigna radiata*, *Taraxacum officinale* and *Sesbania grandiflora* extracts [26–29]. In addition to this, the titanium dioxide that was fabricated with *Euphorbia prostrata* and *Hibiscus rosa-sinensis* experienced polydispersed nanostructures which is an unwanted result from the synthesis process [30,31].

Preprints (www.preprints.org) | NOT PEER-REVIEWED | Posted: 17 February 2021 doi:10.20944/preprints202102.0380.v1

3.2. Iron and Iron Oxide Nanoparticles

A study conducted by Hoag et al. (2009) was one of the first recorded articles for the green synthesis of zero valent iron nanoparticles. Their research utilises the polyphenols in *Camellia sinensis* to act as the bioreducing agent for different salts of iron such as $FeCl_3$, $FeSO_4$ and Fe-EDTA at room temperature. The characterisation techniques using TEM, UV and XRD to identify the nanostructures. It was found that the zero valent iron were spherical in nature and possessed diameters ranging from 5-15 nm.

Similarly, Latha & Gowri (2014) published their findings on the synthesis of magnetite (Fe_3O_4) using the aqueous extract of *Caricaya papaya* leaves. The SEM images of the nanomaterial indicated the morphology plate-like structures with coarsened grains and capsules; whilst, from the XRD analysis, it was found that the average particle size of the magnetite was 33 nm. Furthermore, Pravallika et al. (2019) recently studied the green synthesis of iron oxide nanoparticles using the extract of *Centella asiatica* by reducing ferrous and ferric chlorides. The TEM image of the nanopowder displayed agglomerated spherical shaped particles ranging from 20-40 nm in size. According to the FTIR analysis, it was confirmed that the nanostructures were capped with biomolecular compounds such as triterpenoids.

In addition to the above, iron nanoparticles were synthesised by using *Lawsonia inermis* and *Gardenia jasminoides* extract in a study conducted by Naseem & Farrukh (2015). The TEM results obtained from the *Lawsonia inermis* extract displayed a particle size of 21 nm, while the latter extract's iron nanoparticles were observed to be 32 nm. The SEM images of the extracts exhibited agglomerated nanostructures with hexagonal and shattered rock-like appearances for *Lawsonia inermis* and *Gardenia jasminoides* extracts, respectively. Moreover, Yuvakkumar et al. (2014) synthesised magnetite (Fe_3O_4) nanoparticles using *Nephelium lappaceum* waste extract as a green ligation and chelating agent. The XRD study discovered that the iron oxide nanoparticles possessed a spinel structure, while the TEM images revealed an average particle size of 200 nm.

The synthesis of nanoparticles of iron nanoparticles and their oxides were strongly influenced by the concentration of antioxidant compounds within the various plant extracts used, where the plants with high phenolic content were found to display the greatest reductive capabilities [37,38]. Despite the aforementioned anomalies in the morphologies of the nanoparticles, the majority of the shapes were discovered to be spherical, with the average size of iron and iron oxide nanoparticles was found to be approximately 58 nm (Table S7). Additionally, numerous researchers experienced agglomeration as seen in the TEM and SEM images of the nanomaterial [39,40].

3.3. Cobalt and Cobalt Oxide Nanoparticles

In 2015, a study conducted by Sharma and co-authors displayed the successful synthesis of Co_3O_4 nanoparticles using the aqueous extract of *Calotropis gigantea* leaves. From the SEM and TEM results, Sharma and co-authors (2014) observed nearly spherical shaped particles with diameters ranging from approximately 60-80 nm. The EDX spectrum found Co and O to be the major elements, which indicates the cobalt oxide nanoparticles were of high purity.

Interestingly, Han and co-authors (2015) established the green synthesis of three-dimensional hierarchical porous cobalt oxide nanostructures by using mature *Gingko biloba* leaves as a growth template. After thoroughly rinsing the plant material with water, and drying at 60°C for 3 hours, the leaves were introduced in 0.1 M cobalt(II) acetate ($Co(CH_3COO)_2$) solution where the mixture was left at room temperature overnight. The proposed reaction for the reduction of the cobalt salt is displayed in Equation 1. From the TEM and SEM images, it was deduced that the nanoparticles possessed a hierarchical, porous worm-hole-like structure with sizes ranging from 30-100 nm.

$$3Co(CH_3COOH)_3 + 8O_2 \rightarrow Co_3O_4 + 12CO_2 \quad (1)$$

Furthermore, cobalt nanoparticles were synthesised using the biomolecules extracted from *Conocarpus erectus* [43]. In the study's methodology, the extraction process took place using 100 g of the powdered leaves in 500 mL of methanol, ethanol and deionised water, separately. It was found that the methanolic extract contained a higher concentration of total phenolic compounds (296 µg/g), which is considered to be the main contributor to the antioxidant capacity of the plant. Therefore, methanol was used as the primary solvent for the experimental investigation. The SEM results disclosed cobalt nanoparticles possessing spherical morphologies and diameters ranging from 20-60 nm.

Other interesting morphologies such as octahedral, hexagonal, pentagonal, plate-like and spinel were obtained through the use of *Manihot esculenta crantz*, *Chromolaena odorata*, *Mangifera indica*, *Helianthus annus* and *Moringa oleifera*, respectively (Table S8) [44–48]. Additionally, the average nanoparticle size of the cobalt-based materials was found to be approximately 54 nm, with multiple studies experiencing agglomeration [49,50]. Moreover, Diallo abd co-authors (2015) discovered that phenolic compounds exhibit high antioxidative properties and were the major contributors to the reduction of metal ions, whereas plants with high concentrations of proteins, lipids and amino acids contribute to stabilising the nanostructures and, in turn, inhibits the formation of agglomerates.

3.4. Nickel and Nickel Oxide Nanoparticles

One of the first recorded studies that utilised plant extract for the synthesis of nickel nanoparticles was conducted by Sudhasree and co-authors (2014). Their research employed the aqueous extract of *Desmodium gangeticum* root, where the extraction process was conducted using the Soxhlet method and amounting to a concentration of 1 mg/mL. The ultraviolet-visible spectrophotometer confirmed the synthesis of nickel nanoparticles with a sharp band at 270 nm, with the morphology found to be spherical and monodispersed. Another study utilised *Camellia sinensis* as a reducing and capping agent for the synthesis of nickel nanostructures [53]. The SEM images of the nanostructures displayed spherical shapes with an average particle size of 42 nm.

Nickle oxide nanoparticles were synthesised via the green route using *Aloe vera* by Juibari & Eslami (2019). The SEM results displayed the morphology of nanorods with homogenous structures with an average diameter of 50-70 nm. Furthermore, nickel oxide nanoparticles were prepared using *Physalis angulata* leaf extract in in recent experimentation conducted by Sulaiman & Yulizar (2018). The XRD investigation showed different diffraction peaks at 37.31°, 62.82°, 75.42° and 79.56° which corresponds to index (111), (200), (220), (311) and (222), respectively. The crystalline structure was cubic and had an average size calculated to be approximately 7.08 nm. The electron microscope studies displayed the morphology of spherical particles, whilst the particle size analysis found a homogenous size distribution with a sharp peak at 64.13 nm. The vibration spectroscopy reported the typical metal-oxygen stretching vibration at 419 cm^{-1} and 913 cm^{-1} due to the presence of NiO nanostructures. In addition, slight hydration could be observed since broad bands peak at 3510 cm^{-1} and 1654 cm^{-1}.

Nickel nanoparticles were confirmed to possess superparamagnetic properties at ambient temperatures, with the majority of the studies retaining spherical morphologies and face centred cubic structures that possessed an average diameter of 34 nm (Table S9) [56]. Once again, aggregation of the nanostructures was an issue for researchers during the synthesis of these nickel-based compounds which may have been caused by the presence of cell components on the surface of nanoparticles or due to magnetic interaction and polymer adherence between the particles [57–61]. Additionally, a study conducted by Chen and co-authors (2014) mentioned that the flavonoids and sugars of alfalfa extract were the main reducing agents for Ni(II), confirming the involvement of these phytochemicals during the reduction process.

Preprints (www.preprints.org) | NOT PEER-REVIEWED | Posted: 17 February 2021 doi:10.20944/preprints202102.0380.v1

3.5. Copper and Copper Oxide Nanoparticles

Nasrollahzadeh and co-authors (2014) reported the synthesis of copper nanoparticles using the aqueous extract of the *Euphorbia esula* leaves. The morphology of the nanomaterial was found to be spherical with the sizes distributed in the range of 20-110 nm, according to the TEM images. Similarly, *Phyllanthus embilica* plant extract was previously used to synthesise copper nanostructures [64]. The synthesis procedure involved the introduction of the extract to 0.1 M sodium hydroxide (NaOH) under constant stirring, where a colour change from white to yellowish green was observed. It was found that increasing the temperature of the solution to 80°C altered the colour to brown, indicating the formation of the nanoparticles. The SEM results exhibited the shape of the nanoparticles to be flake-like with diameters ranging from 15-30 nm.

Furthermore, Veisi and co-authors (2017) confirmed the biosynthesis of copper oxide nanoparticles using *Thymbra spicata* leaves extract. The morphological studies displayed the formation of homogeneous and relatively spherical copper oxide particles without agglomeration in the size range of 10-20 nm. The XRD analysis confirmed the presence of CuO nanostructures and displayed high crystallinity. Moreover, the green synthesis of copper oxide nanostructures was investigated using *Ocimum basilicum* extract by Altikatoglu and co-authors (2017). The FTIR spectroscopy was used to identify the functional groups based on the bands from the scan. The peak at 3393 cm^{-1} was attributed to the O-H stretching vibrations of alcohols and phenols. The bands situated at 1600 and 510 cm^{-1} formed due to the stretching of Cu-O, which confirms the synthesis of copper oxide nanoparticles. In a recent study, Jayarambabu and co-authors (2020) successfully synthesised copper nanostructures by using the aqueous extract of *Curcuma longa*. The production of the extract consisted of 10 g of the powdered leaves in 100 mL of ethanol for 4 hours at 70°C. The mixture was then added to 100 mL of 0.1 M copper acetate dihydrate and kept in a microwave for 180 s at 200 W power. The high resolution FESEM and TEM images displayed particles with spherical morphologies with diameters ranging from 5-20 nm.

Copper and copper oxide nanoparticles were found to possess mainly spherical shapes with an average size of 53 nm (Table S10). Numerous researchers conducted FTIR characterisation techniques on the extract solutions and the biosynthesised nanostructures which found that the reduction of the metallic ions was a result of the phytochemicals such as phenols, flavones, terpenoids, proteins and other heterocyclic compounds present during the reaction [68–71]. Initial agglomeration of the nanoparticles was reported in numerous studies, where aggregation also increased after a period of time [72,73]. However, it was denoted that the agglomeration may have been caused by an increase in catalytic activity on the surface of the nanoparticles, leading to the enhancement of its application [74].

Preprints (www.preprints.org) | NOT PEER-REVIEWED | Posted: 17 February 2021 doi:10.20944/preprints202102.0380.v1

3.6. Zinc and Zinc Oxide Nanoparticles

A study conducted by Sangeetha and co-authors (2011) was one of the first reported green synthesis of zinc oxide using plant extract. The research utilised *Aloe barbadensis miller* leaf extract as a reducing and capping agent for the desired metallic salt. Firstly, the extract solution was prepared by washing 250 g of the *Aloe* plant and boiling in deionised water. Different concentrations of the extract were formulated using dilution with distilled water, which totalled a volume of 250 mL. Thereafter, zinc nitrate ($Zn(NO_3)_2$) was dissolved in the extract solution under vigorous stirring at 150°C for 5-6 hours. The SEM and TEM monographs displayed ZnO nanoparticles that were agglomerated with spherical and hexagonal morphologies and particle sizes ranging from 25-55 nm.

Correspondingly, Qu and co-authors (2011) successfully synthesised zinc oxide nanoparticles from the aqueous extract of *Physalis alkekengi*. The TEM image showed that the nanostructures were polydispersed with triangular and elongated morphologies ranging from 50-200 nm diameters. Furthermore, zinc oxide nanoparticles were formulated using the aqueous extract of *Lantana aculeata* leaf [77]. The UV-vis spectrum of the nanomaterial recorded a peak at 362 nm, which confirms the presence of ZnO nanoparticles. The FTIR studies further confirmed the successful green synthesis of the metal oxide nanomaterial, with the peak at 443.63 cm^{-1} allotted to ZnO, caused by the stretching of the zinc and oxygen bond. The remaining peaks at 1028.06, 1097.5, 1757.15 and 3481.51 cm^{-1} were due to the presence of the compounds amongst the nanostructures. These include aliphatic amines, carboxylic acids, alcohols and phenols. The morphological analysis carried out on the substance displayed FESEM and HRTEM images with spherical ZnO particles and an average size of 12 ± 3 nm.

The majority of the studies utilised the green synthesis method to fabricate zinc oxide nanoparticles rather than pure zinc nanostructures. However, zinc nanoparticles were successfully synthesised through the use of *Andrographis paniculata*, *Cestrum nocturnum*, *Solanum nigrum* and *Spilanthes acmella* extracts which produced spherical and wire-like morphologies with particle sizes of ranging from 10-70 nm [78–81]. The average particle size of zinc-based nanostructures was found to be approximately 44 nm and possessed spherical morphologies with hexagonal structures (Table S11). Other interesting morphologies such as floral, cylindrical and sponge-like shapes were obtained by using *Phyllanthus emblica*, *Parthenium hysterophorus* and *Hibiscus rosa-sinensis*, respectively [82–84]. In addition, despite the high purity of the zinc and zinc oxide nanostructures, many researchers discovered their resulting nanoparticles to be agglomerated due to the electrostatic attraction [85–87].

Preprints (www.preprints.org) | NOT PEER-REVIEWED | Posted: 17 February 2021 doi:10.20944/preprints202102.0380.v1

3.7. Palladium and Palladium Oxide Nanoparticles

In 2009, Sathishkumar and co-authors reported one of the first studies that utilised *Cinnamom zeylanicum* extract for the synthesis of palladium nanoparticles. The TEM and XRD analysis confirmed the successful synthesis of palladium nanoparticles with spherical morphologies and diameters ranging from 15-20 nm. In addition, *Moringa oleifera* extract was used in the microwave assisted green synthesis of palladium nanoparticles [89]. For this study, the plants were washed and grinded down to a fine powder, where maceration in methanol and petroleum ether were used as separate solvents for the extraction process. The methanolic extract solution obtained a higher yield than the latter and, therefore, was further used in the production of the nanostructures. Microwaves were utilised to irradiate a mixture of 80 mL of 1 mM palladium acetate ($Pd(OAc)_2$) and 20 mL of the extract at 300 W for 5 minutes. The morphological studies of the nanoparticles revealed agglomerated particles with spherical shapes and an average size of 27 nm.

Moreover, Sharmila et al. (2017) conducted experiments that resulted in the successful synthesis of palladium nanoparticles by utilising the aqueous leaf extract of *Filicium decipiens*. The TEM images displayed spherical shapes with the size distribution of 2-22 nm and a mean particle size of 6.36 nm. Furthermore, palladium nanoparticles were synthesised by using *Origanum vulgare* leaf extract as a bio-reductant [91]. The UV-vis spectral analysis did not show absorption bands at 415 nm due to Pd(II) from the metal salt. Therefore, this indicated the development of Pd(0) nanoparticles. The TEM images of the palladium nanostructures established that the particles possessed spherical morphologies with diameters ranging from 2-20 nm.

The plant-mediated synthesis of palladium oxide nanoparticles has not yet been extensively explored and only one investigation using *Aspalathus linearis* was discovered [92]. The metal-oxide nanostructures were characterised and found to possess spherical morphologies with pure tetragonal crystallites and a size range of 3.8-22 nm. Previous research on the biosynthesis of plant-conjugated palladium nanoparticles obtained mostly spherical particles with a mean size of approximately 24 nm, which is relatively small compared to other metallic nanoparticles (Table S12). Additionally, detailed analysis of the plant extracts used for the biosynthesis of palladium nanoparticles indicated that flavonoids, polyphenols, saponins, tannins, anthocyanins, betacyanins, terpenoids, steroids and proteins served as the key donors of electrons during the redox reaction for the fabrication of Pd nanoparticles. These phytochemicals are absorbed onto the surface of the nanostructures through π-electron interactions if other strong ligating agents are not present [90,93,94]. Moreover, agglomeration was another issue faced by researchers, deeming them thermodynamically unstable as they are, by nature, finely divided mass [95,96].

Preprints (www.preprints.org) | NOT PEER-REVIEWED | Posted: 17 February 2021 doi:10.20944/preprints202102.0380.v1

3.8. Silver and Silver Oxide Nanoparticles

In a study conducted by Gopinath and co-authors (2012), silver nanoparticles were biosynthesised using the extract of *Tribulus terrestris*. The TEM and AFM analysis methods determined the size and morphologies of the nanomaterial, with the average particle size being 22 nm that possessed spherical shapes. In addition, silver nanoparticles were synthesised through the bioreduction of the desired metallic salt by the leaves and fruit extracts of *Securinega leucopyrus* [98]. The SEM images of the nanostructures indicated that the particles possessed morphologies from spherical to oval shapes; while the TEM analysis shows the particle size range within 11-20 nm. Similarly, aqueous *Rubus glaucus* extract was utilised to synthesis silver nanoparticles in research conducted by Kumar and co-authors (2017). The morphological studies carried out by the TEM analysis method found that the particles retained a predominantly spherical shape, with average diameters ranging from 12-50 nm.

Arokiyaraj and co-authors (2017) successfully biosynthesised silver nanoparticles by using the aqueous leaf extract of *Rheum palmatum*. The SEM and TEM images of the compound showed that the particles possessed hexagonal and spherical shapes, with sizes ranging from 44-113 nm. Although not as extensively studied as pure silver nanoparticles, silver oxide nanoparticles have been successfully synthesised through the use of plant extracts [101,102]. More specifically, Ravichandran and co-authors (2016) fabricated Ag_2O nanostructures through *Callistemon lanceolatus* extract as a reducing and capping agent. The redox reaction (Equation 2-3) was initiated by mixing 5 mL of the aqueous extract with 100 mL of 1 mM $AgNO_3$ and incubated at 37°C for a period of 1-3 hours. The nanomaterial was characterised using UV, EDX, XRD and HRTEM techniques, which resulted in the discovery of spherical and hexagonal morphologies, with particle sizes ranging from 3-30 nm.

$$Ag^+ + OH^- \rightarrow AgOH \quad (2)$$

$$2AgOH \rightarrow Ag_2O + H_2O \quad (3)$$

The biosynthesis of silver nanoparticles has been generously studied over the past decades, with the majority of the nanostructures resulting in spherical morphologies and an average diameter of 41 nm (Table S13). However, numerous researchers encountered silver nanoparticles that were aggregated and polydispersed [104–106]. Furthermore, Alghoraibia and co-authors (2019) confirmed that the total phenolic content in the extract solution was directly related to the antioxidant capacity, where a higher concentration of phenolic compounds will produce a stronger reduction of metallic ions [108].

Preprints (www.preprints.org) | NOT PEER-REVIEWED | Posted: 17 February 2021 doi:10.20944/preprints202102.0380.v1

3.9. Platinum Nanoparticles

The aqueous leaves extract of *Quercus glauca* was reportedly used for the rapid and eco-friendly synthesis of platinum nanoparticles by Karthik and co-authors (2016). The UV-vis spectroscopy of the metallic salt precursor and extract solution displayed peaks at 217 and 273 nm, respectively; these wavelengths diminished with an increase in the absorption value, which confirmed the complete reduction of Pt (IV) ions to Pt nanostructures. The TEM data provided the morphological details of which indicated that the platinum nanoparticles had a nearly spherical shape, with particle sizes ranging from 5-15 nm.

A bio-synthetic green route using *Xanthium strumarium* leaf extract for the synthesis of platinum nanostructures was developed by Kumar and co-authors (2019). The study utilised 2 g of the fresh leaves that were ground to a fine powder and mixed with 200 mL deionised water and boiled for 30 minutes. The extract solution was then introduced into 190 mL of 1 mM aqueous $H_2PtCl_6.6H_2O$ to complete a volume of 200 mL, where the reaction temperature was increased from room temperature to 100°C and left for 1 hour. The SEM and TEM images showed that the nanostructures possessed a smooth surface, good alignment and were free from distortion, with cubic to rectangular shapes and an average size of 20 nm.

Furthermore, Tahir and co-authors (2017) utilised the aqueous extract of the medicinal plant *Taraxacum laevigatum* for the green synthesis of platinum nanoparticles. The nanoparticles were successfully synthesised due to the confirmation sought out by the UV-vis spectroscopy, with the peak originating at 283 nm. The morphological studies resulted in the discovery of the nanoparticles being dispersed, spherical and uniformly sized with an average particle size of 2-7 nm. Moreover, the biomimetic synthesis of platinum nanoparticles, conducted by Ganaie and co-authors (2018), was accomplished through the utilisation of the terrestrial weed *Antigonon leptopus*. The electron microscopic studies determined that the nanoparticles formed were predominantly spherical, with sizes varying from 5-190 nm.

After conducting thorough research through previous studies, it is believed that there has been attempt to biologically synthesise of platinum oxide nanoparticles. Additionally, platinum nanostructures possess the smallest average diameters between the transition-metals examined in this review, with it being approximately 21 nm (Table S14). The majority of the nanoparticles retained spherical shapes, however, some studies produced rod-like, wire-like, dodecahedron, hexagonal and rectangular morphologies [110,113–116].

3.10. Gold Nanoparticles

One of the first reported green synthesis of gold nanoparticles was conducted by Kumar and co-authors (2011), which utilised *Zingiber officinale* extract as a bioreducing and capping agent. The UV-vis spectroscopy confirmed the formation of the gold nanostructures with a surface plasmon resonance (SPR) band emerging at approximately 523 nm. The DLS study obtained a size distribution curve which revealed the majority of the particle sizes were found to be in the range of 4-13 nm. Moreover, aqueous *Cassia auriculata* leaf extract was used in the facile green synthesis of gold nanoparticles [118]. The TEM results displayed spherical, hexagonal and triangular particle shapes, with sizes ranging from 15-25 nm.

Dubey and co-authors (2010) conducted their research by using the aqueous leaf extract of *Sorbus aucuparia* for the development of gold nanocolloids. The study administered 45 g of the thoroughly washed leaves in 180 mL of ultrapure water and boiled the mixture for 15 minutes. An aqueous solution of 10^{-3} M auric acid ($HAuCl_4$) was then reduced through the addition of 1 mL of the leaf extract at room temperature for 15 minutes, as seen in equation 4 [120].

$$4H^+[Au^{3+}Cl_4]^- + 12H^+ + 12e^- \rightarrow 4Au^0 + 16HCl \quad (4)$$

The XRD studies of the substance resulted in peaks at 38.21°, 44.39°, 64.62°, 77.59°, 81.75°, 98.16°, 110.89° and 115.27° which is attributed to the face centred cubic structure of gold

Preprints (www.preprints.org) | NOT PEER-REVIEWED | Posted: 17 February 2021 doi:10.20944/preprints202102.0380.v1

nanoparticles. Using the Debye-Scherrer equation and the isolated peaks at (111), (311) and (420), the average crystallite size was calculated to be 18 nm. Furthermore, The biosynthesis of gold nanoparticles using the leaf extract of *Terminalia catappa* was carried out in a study conducted by Ankamwar (2010). The UV-vis absorption spectra recorded the SPR vibrations in the gold nanostructures at a wavelength of 524 nm, therefore, establishing the existence of the desired nanoparticles. The morphological studies of the nanocolloids derived that the particles were predominantly spherical, with sizes ranging from 10-35 nm and an average size of approximately 21.9 nm.

Once again, the antioxidant capacity of plant extracts was found to be highly dependent on the concentration of phenolic compounds and other phytochemicals present, as these biomolecules are considered to be the major contributors to the plants' reductive capabilities due to their adaptation in response to biotic and abiotic stresses [122]. Additionally, gold nanoparticles were mostly mono-dispersed and possessed spherical morphologies with an average particle size of 45 nm (Table S15). On the other hand, there were numerous studies that experience different shapes which include triangular, pentagonal and hexagonal morphologies [123–125]. Furthermore, polydispersity and the clustering of particles were the main obstacles faced by researchers during the biosynthesis of gold nanoparticles [126,127].

4. Factors Affecting the Green Synthesis of Nanoparticles

The following section will cover the various parameters that have been previously discovered to affect the characteristics of green synthesised nanoparticles. These include factors such as concentration, reaction temperature, contact time, pH level, and calcination temperature. With analysing how the size and morphologies react to the different parameters, it may be possible to tweak the process in order to obtain the desired characteristics of the nanoparticles for future researchers.

4.1. Concentration

In a study conducted by Anigol and co-authors (2017), silver nanoparticles were synthesised through the use of *Capparis moonii* aqueous extract as a bioreducing and capping agent. The research employed various concentrations of a silver nitrate solution that was mixed with the extract. More specifically, 250 mL of 1 mM, 2 mM, 3 mM, 4 mM and 5 mM $AgNO_3$ solution were separately mixed with 50 mL of the extract and microwaved for 30 minutes while maintaining a constant volume. As seen in Figure 3d, the nanostructures were characterised by using the UV-vis spectrum which displayed a surface plasmon absorption band at 430 nm. A general trend was found of which the SPR peak shifted towards the higher wavelength region and became narrower as the concentration increased. This shift in wavelength was accompanied by a decrease in the nanoparticle diameter, however, this contradicts other studies that have stated a red shift denotes an increase in particle size or agglomeration [126,129,130]. In addition, the broadening of the absorption band indicates the existence of a larger size range within the solution. It was concluded that an increase in the metal salt concentration resulted in the formation of nanostructures of a smaller diameter.

Similarly, the aqueous extract of *Citrus paradisi* was utilised in the biosynthesis of silver nanoparticles [131]. In the experiment conducted, different volumes of the plant extract and silver nitrate (1 mM) solution were used to vary the concentrations of the synthesis procedure. This was accomplished by accurately measuring the volumes and mixing the plant extract and metallic salt solutions in ratios of 50:50, 40:60 and 20:80, respectively. The reactions were carried out in sunlight for 30 minutes, where a colour change was then observed. The nanoparticles were characterised and determined to have spherical morphologies, with a size range of 5-65 nm and a mean size of 55.02 nm. The UV-vis analysis of the nanomaterial solution, seen in Figure 3a, displayed no absorption bands for the 40:60 and 50:50 concentrations; however, the 50:50 volume ratio did reveal a stronger absorbance than the 40:60 ratio. On the other hand, the 20:80 volume ratio displayed an intense, broad peak with

Preprints (www.preprints.org) | NOT PEER-REVIEWED | Posted: 17 February 2021 doi:10.20944/preprints202102.0380.v1

the maximum absorption rate being at 420 nm. Faghihi and co-authors (2017) suggested that the higher absorption indicated the increased formation of silver nanoparticles. Therefore, this suggests that the optimal reaction mixture should mainly consist of a higher metal salt concentration, rather than the extract concentration. On the contrary, Asemani & Anarjan (2019) obtained different results, with the optimal ratio having 1 g of ions in 40 mL of 0.05 g/mL extract solution, despite the use of 4 g of the metallic salt; therefore, the larger part of the mixture consisted of the extract.

The green synthesis of zinc oxide nanoparticles was performed by utilising *Prunus avium* extract [133]. The effect of concentration of the metal salt solution was studied, where 10 mL of the extract solution was introduced into four separate beakers containing 30 mL of zinc nitrate hexahydrate ($Zn(NO_3).6H_2O$) with differing concentrations of 0.005 M, 0.02 M, 0.05 M and 0.3 M. The reaction was kept at room temperature and stirred at 150 rpm for 30 minutes, then incubated for 12 hours. The nanostructures were characterised through UV, SEM, XRD and FTIR techniques, which confirmed high-purity zinc oxide nanoparticles with hexagonal shapes and an average size of 20.18 nm. Mohammadi & Ghasemi (2018) stated that when the zinc ion concentration was increased, the lower quantities of hexagonal structures formed with an average size of 20.7-96.5 nm due to the formation of large anisotropic particles (Figure 3f). This may have been caused by keeping the plant extract volume constant, as the phytochemicals are responsible for the capping and stabilisation of the nanoparticles. It was concluded that the zinc nitrate concentration of 0.005 M was optimal as there were more functional groups for the zinc ions to interact with [134]. On the other hand, increasing the concentration resulted in the formation of larger particles and aggregations due to the competition between the zinc ions and phytochemicals for nucleation of the nanostructures.

Kumar and co-authors (2017) demonstrated the successful synthesis of silver nanoparticles through the utilisation of *Prunus persica* extract. The nanostructures were prepared by adding 10 mL of a 0.01 M $AgNO_3$ into five different volumes of plant extract solution, namely, 1.0 mL, 2.0 mL, 3.0 mL, 4.0 mL and 5.0 mL. The reaction was maintained at room temperature, where a colour change from yellow to brown was observed after 5 minutes, indicating the formation of silver nanoparticles. Kumar and co-authors (2017) established that the silver ions above a particular concentration limit may be toxic to the secondary metabolites as they may cause precipitation. However, the precipitation is prevented as the ionic forms are transformed into nanoparticles. It was found that as the concentration of the plant extract was increased, the absorbance of the sample generally decreased. This was an indication of an increase in the size of the silver compounds which was confirmed through various characterisation techniques. More specifically, increasing the concentration coherently reduced the size of the particles until, beyond a certain concentration, the particle sizes increased (Figure 3c & e). It was also mentioned that a higher ratio of reducing agent to substrate accelerates the reduction of Ag^+ to Ag^0 but diminishes the quality of the nanocomposites.

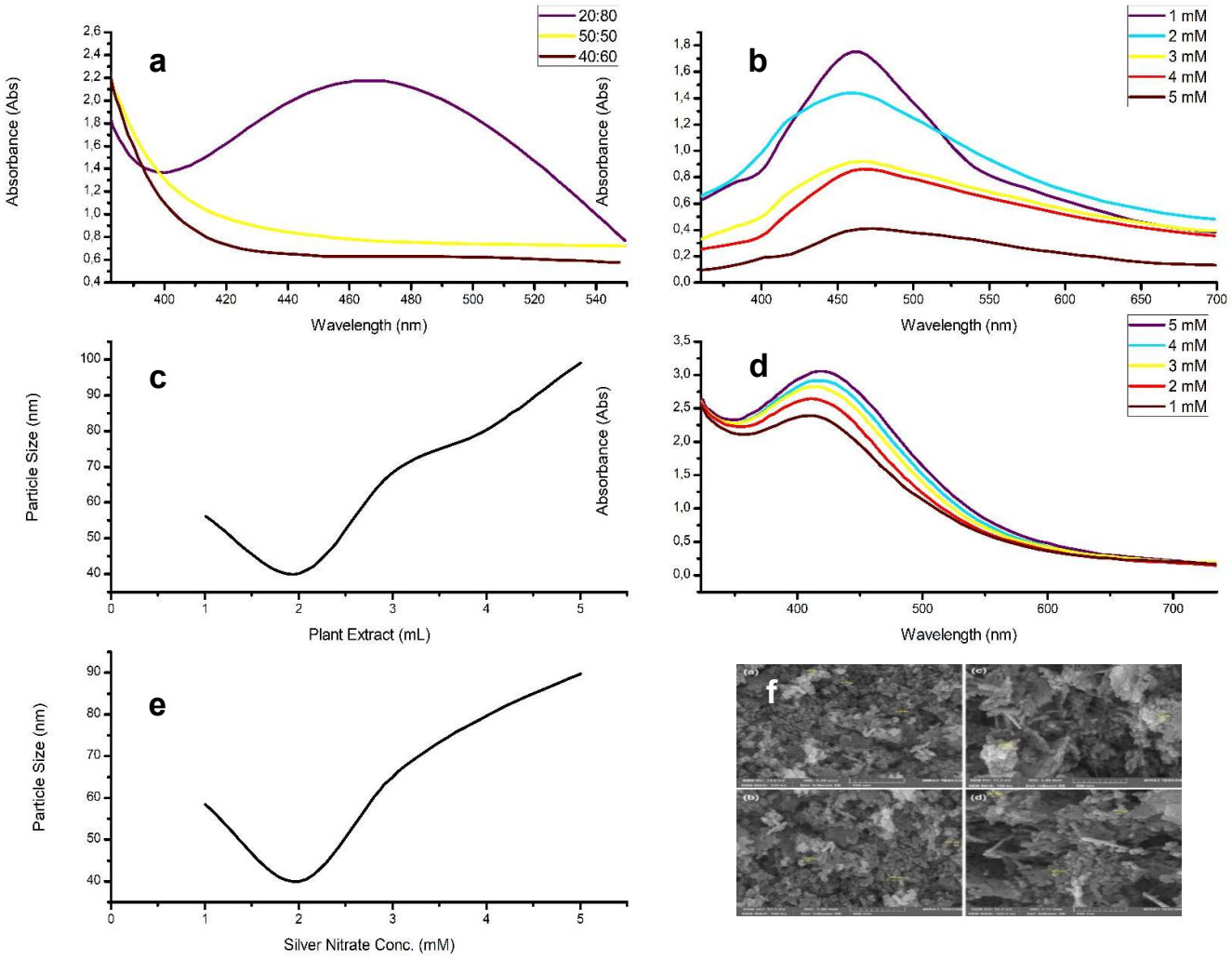

Figure 3: The readapted graphs of, a) The effect of plant extract to metal salt ratio on Citrus paradise-mediated AgNPs [131]*; b) The UV-vis spectra of varying concentrations of $AgNO_3$ in the synthesis of AgNPs from Coleus aromaticus extract* [134]*; c) The effect of Prunus persica extract volume on AgNP diameter* [150]*; d) The UV-vis spectrum of different $AgNO_3$ concentrations on Capparis moonii-conjugated AgNPs* [128]*; e) The effect of $AgNO_3$ concentration on Ag nanoparticle size fabricated through Prunus persica* [150]*; f) SEM of Prunus avium-mediated ZnO nanoparticles using different zinc nitrate concentrations* [133].

Preprints (www.preprints.org) | NOT PEER-REVIEWED | Posted: 17 February 2021 doi:10.20944/preprints202102.0380.v1

4.2. Reaction Temperature

The effect of synthesis temperature was studied during the growth of silver nanoparticles using *Vitex agnus-castus* aqueous extract [136]. The reaction was kept under continuous stirring for various periods of time at temperatures of 40-80°C. The formation of the nanomaterial was monitored by measuring the intensity of the SPR band in the UV-vis spectra, which resulted in the maximum absorption band positioned at 420 nm due to the presence of silver nanostructures. There were clear differences in the surface plasmon resonance band as the temperature was altered; however, large differences could only be observed after a reaction period of 2 hours. Since the SPR peak is inversely proportional to the diameter of the nanoparticles, it was estimated that the colloids synthesised at 40°C were smaller than 1 nm; thus, the particles may not have possessed sufficient stability. The UV-vis absorption peaks increased as the temperature increased from 50°C to 80°C, with the fastest formation of the nanoparticles occurring at the highest temperature utilised. For the lower temperatures, a slower increase in the absorption band was observed, indicating a delayed particle growth. It was concluded that the rate of nanostructure formation was strongly temperature-dependent, with the optimal temperatures being 60°C to 80°C. This was assumed to be caused by the larger phytochemicals from the biomatter that form the organic coating on the surface of the particle which hinders or necessitates higher temperatures for growth.

Furthermore, a study conducted by Latif and co-authors (2018) conducted experiments on the green synthesis of gold nanoparticles with the use of *Centella asiatica* extract as a bioreducing and stabilising agent. The extract solution was produced and 8% was introduced into a 0.5 mM gold chloride ($HAuCl_4$) aqueous solution in equal volume, while using process temperatures of 25°C, 40°C, 55°C and 70°C under constant stirring. The results displayed a low and broad SPR absorption band for the reaction carried at 25°C, where it shifted to 542 nm for 40°C and 536 nm for 55°C and 70°C with an increased intensity of sharp and narrow peaks that revealed an increase in sphericity of the particles (Figure 4a). Latif and co-authors (2018) deduced that the temperature has a direct effect on the reaction rate as the consumption of gold ions increases, thereby enhancing the formation of nuclei. It was also suggested that the higher temperatures increase the activation energy of the molecules, therefore leading to a faster reaction rate. In addition, the majority of the gold ions are consumed in the nucleation process, hence the high reaction rate; thus, stalling the secondary reduction on the surface of the preformed nuclei which results in a large population of spherical particles.

In a different experiment, *Cinnamomum camphor* aqueous extract was used in the biosynthesis of silver nanoparticles by Liu and co-authors (2017). The nanostructures were synthesised in two parts with a silver nitrate solution, one with sufficient Ag^+ precursor and the other with insufficient Ag^+ precursor. The researchers evaluated how the temperature of the reaction affected the size of the nanocolloids by altering the temperature of the mixture from 70°C to 90°C, with increments of 5°C. Initially, the study determined the kinetics of the process, with k_1 being the nucleation rate constant and k_2 being the growth rate constant. It was observed that k_1 increases slightly when the temperature was raised from 70°C to 80°C (Figure 4c). On the other hand, this constant becomes relatively sensitive and rises sharply when temperatures exceed 80°C. In addition, the growth rate constant increases linearly as the temperature increases. This should not be the case as higher temperatures are hypothesised to produce smaller nanoparticles. Liu and co-authors (2017) then stated that the phenomenon was caused by either increasing the temperature to above the special value of 80°C, or whether the amount of Ag^+ precursor was sufficient or not. Experimentation concluded that, with sufficient precursor, the diameter of the nanoparticles produced would increase almost linearly; while insufficient precursor resulted in a slight increase in particle diameter up to 80°C and experienced a sharp decrease in size thereafter, as growth would be restricted due to the significant use of Ag^+ ions for nucleation, leaving the reaction with lack of Ag^+ ions for development.

Similarly, Jon and co-authors (2019) conducted a study which utilised *Zea mays* extract in the green synthesis of gold nanoparticles. Multiple samples were prepared for the experimentation to be carried out at various temperatures which include 0°C, 5°C, 30°C, 45°C, 75°C and 90°C. As expected, the surface plasmon resonance band had no peak for 0°C and 5°C; therefore, it can be assumed that there was little or no formation of gold nanostructures. On the other hand, the UV-vis spectrum displayed strong peaks that narrowed and intensified as the temperature increased from 30°C to 75°C which indicated that the size range of gold nanoparticles decreased due to an increase in nucleation. Interestingly, this study displayed similar results to the research conducted by Liu co-authors (2017), as the intensity of absorption band significantly decreased and simultaneously broadened which may have been caused by insufficient ions present in the solution; ultimately, indicating an increase in the size range of the nanostructures [140].

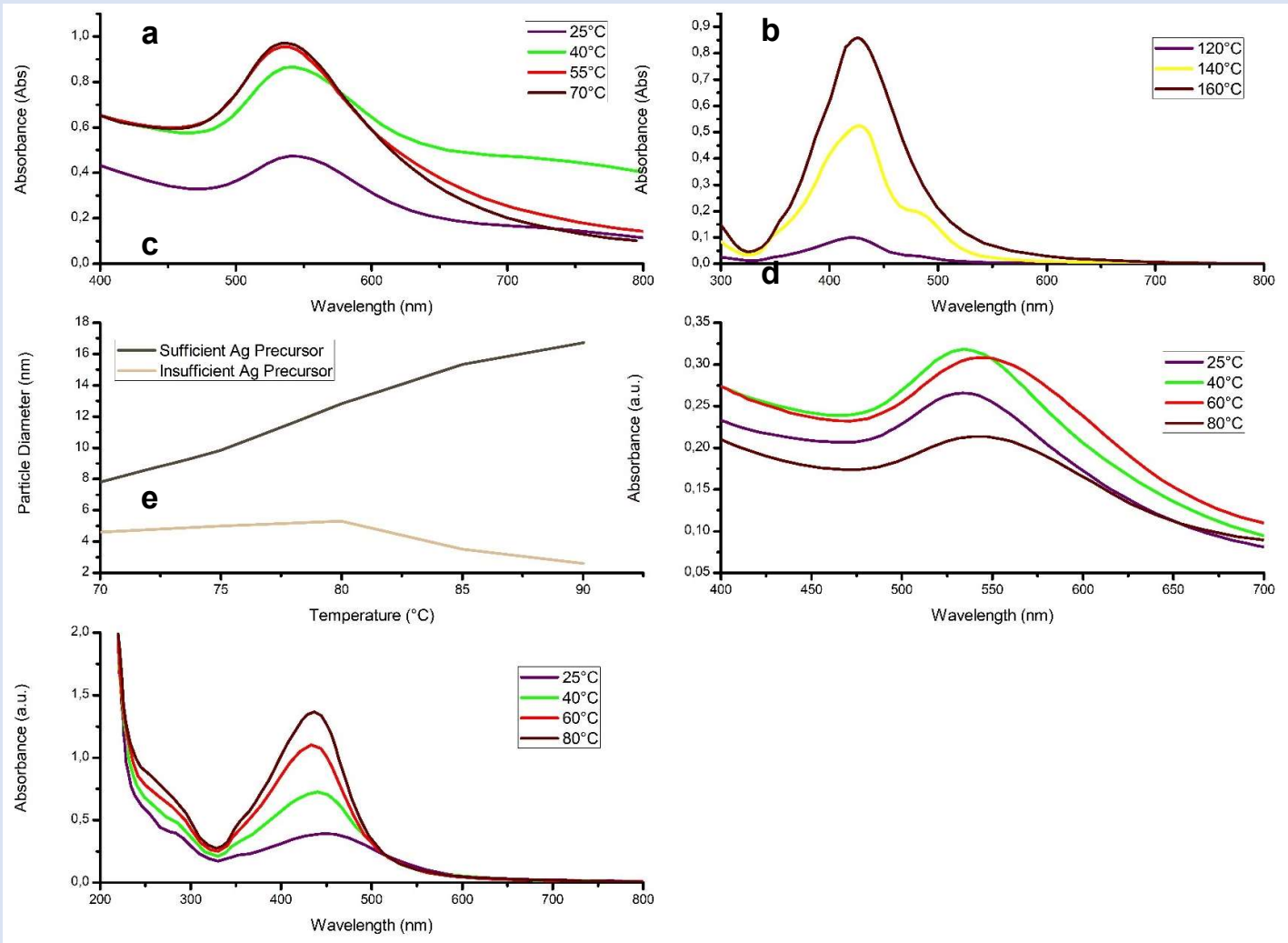

Figure 4: Readapted graphs displaying, a) The UV-vis spectrum of Centella asiatica-mediated AuNPs at different temperatures [137]*; b) The effect of varying synthesis temperatures of green AgNPs* [151]*; c) The effect of different temperatures with sufficient and insufficient precursor on the size of Cinnamomum camphor-mediated AgNPs* [138]*; d) The UV-vis spectra of AuNPs synthesised using Chenopodium formosanum extract through varying the process temperatures* [152]*; e) The effect of different temperatures on Eriobotrya japonica-conjugated AgNPs* [153].

Preprints (www.preprints.org) | NOT PEER-REVIEWED | Posted: 17 February 2021 doi:10.20944/preprints202102.0380.v1

4.3. Contact Time

The effect of reaction time was evaluated during the green synthesis of silver nanoparticles in a study conducted by Ramli and co-authors (2014). The biosynthesis of the silver nanostructures was executed through the addition of 10 mL of *Elaeis guineensis* extract into 90 mL of 5 mM $AgNO_3$ solution, where the mixture was allowed to react under ambient conditions. The researchers investigated the effect of the reaction time by analysing samples through the UV-vis spectrum every 15 minutes for 4 hours (Figure 5d). The UV-vis analysis of the samples displayed a maximum at 435 nm, and the intensity of the band increased as the time progressed. Initially, the rate of change in absorbance was miniscule for the first 45 minutes, where it then increased rapidly up to 120 minutes. The absorption peaks from 120 minutes to 240 minutes were identified to be considerably similar; therefore, Ramli and co-authors (2014) concluded that increasing the reaction time will increase the rate of reduction of silver ions, until the reaction reaches completion.

Behravan and co-authors (2019) accomplished the facile green synthesis of silver nanoparticles through the use of *Berberis vulgaris* leaf and root extract. The nanocompounds were synthesised by adding 3 mM of $AgNO_3$ solution into 5 mL of the aqueous plant extract and placed onto a shaker at ambient temperature for different time periods which include 1, 2, 6, 12 and 24 hours. The investigation of the samples was carried out by the UV-vis spectrum between 200 and 800 nm. It was found that after 1-hour, suspended particles had indeed been generated as a broad peak was observed at approximately 440 nm. Interestingly, the UV-vis results from 2 hours and 6 hours displayed a decrease in the absorption peak intensity (Figure 5a). The authors of this research attributed this phenomenon to the reaction having sufficient contact time for the particles to grow, thus, leading to the reduction in the peak intensity. Thereafter, the analysis at 12 hours and 24 hours increased substantially compared to the previous peaks at 1, 2 and 6 hours. These two peaks were similar in absorbance, indicating that the reaction had reached equilibrium by 12 hours.

Furthermore, *Musa paradisiaca* extract was used in a study implemented by Ibrahim (2015), for the biosynthesis of silver nanoparticles. The effect of time on the nanocolloids was studied extensively, with analysis intervals occurring at 3, 5, 10, 15, 20, 25, 30, 45 minutes, 1, 24, 48, 72 and 96 hours (Figure 5b). Visual observations found a colour change of the mixture to yellowish brown within the first 10 minutes and to reddish brown after 1 hour, indicating the reduction of Ag^+ ions. Therefore, Ibrahim (2015) stated that the intensity of the colour was directly proportional to the incubation time of the reaction mixture. The UV-vis spectrophotometer confirmed this, as it displayed a characteristic SPR band for silver nanoparticles at 433 nm that increased over a period of time. Initially, the rate of reaction was slow for the first 45 minutes. Thereafter, the tangible rate was observed until the contact time reached 72 hours, where it achieved the strongest SPR absorption peak and, ultimately, reaction equilibrium. The study concluded that this was due to the increase in the number of silver nanoparticles suspended in the solution.

Therefore, it can be said that the contact time generally increases the overall concentration of the nanomaterial until an equilibrium is reached. Thereafter, the nanostructures may tend to form agglomerates as the nucleation rate decreases and the growth of the nanoparticles continues. Lastly, depending on the nanoparticle being synthesised and the biological medium used, the time taken to reach equilibrium varies.

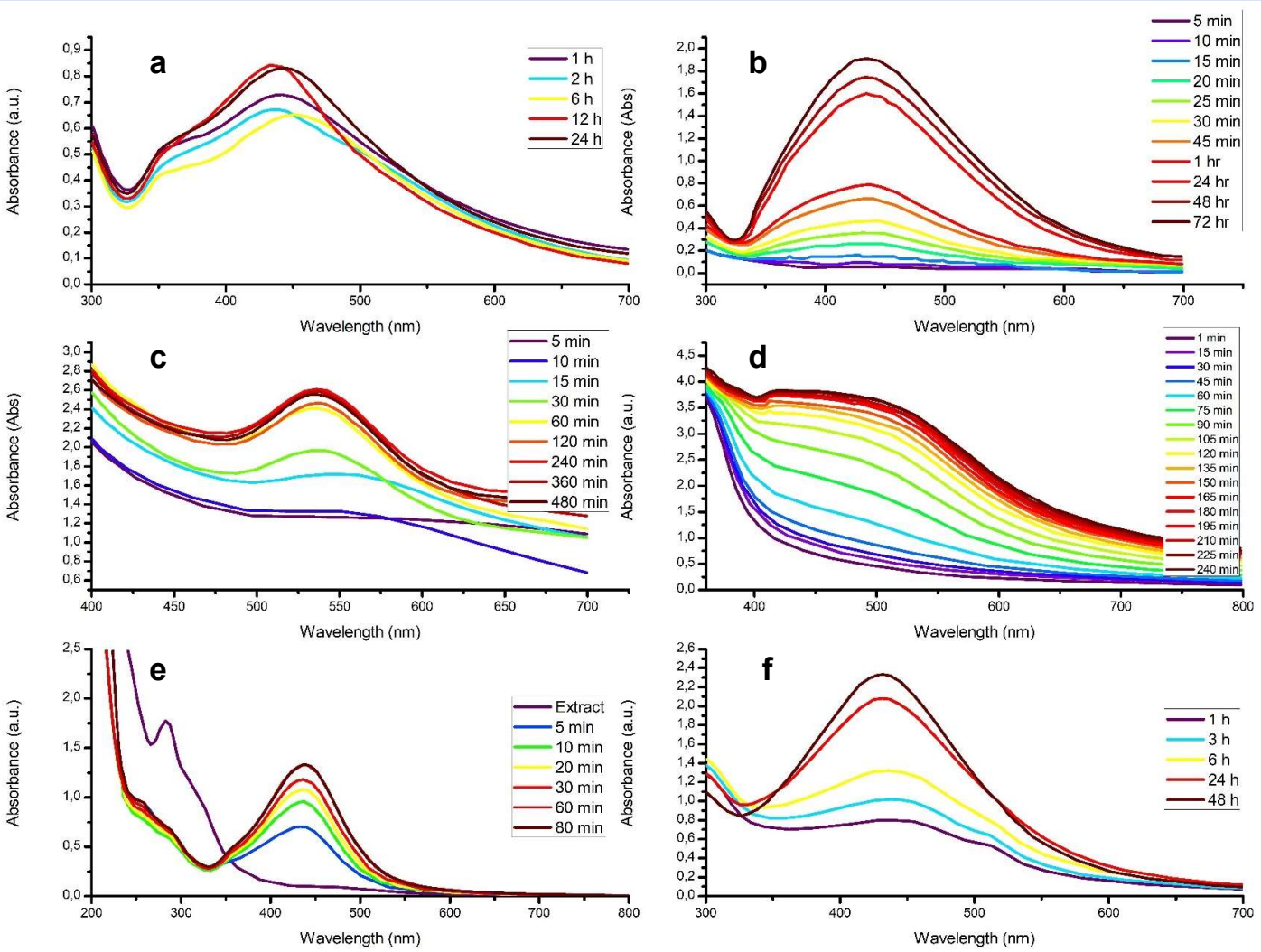

Figure 5: The readapted UV-vis absorption spectrum of, a) silver nanoparticles synthesised from Berberis vulgaris at different reaction times [142]*; b) Musa paradisa-conjugated AgNPs at various time intervals* [143]*; c) the time-dependent synthesis of AuNPs using Elaeis guineensis* [154]*; d) silver nanoparticles biosynthesised using Elaeis guineensis during different time periods* [141]*; e) Eriobotrya japonica-mediated AgNPs at various time intervals* [153]*; f) colloidal AgNPs at different reaction times* [155].

4.4. pH Level

In a study conducted by Singh & Srivastava (2015), gold nanoparticles were synthesised by utilising *Amomum subulatum* aqueous extract as a strong reducing and stabilising agent. The research employed five samples containing 10 mL of 1 mM $HAuCl_4.3H_2O$, where the pH level was altered from 3 to 11 with intervals of 2. The effect of the solution's pH level was examined through the use of a UV-vis spectrophotometer. The investigation found surface plasmon resonance absorption bands at 572, 560, 544, 548 and 562 nm for the pH values of 3, 5, 7, 9 and 11, respectively (Figure 6d). As previously stated, an increase in wavelength is deemed a redshift, which is usually accompanied by an increase in particle size. Therefore, Singh & Srivastava (2015) concluded that the size of the gold nanoparticles decrease as the solution changes from acidic (pH 3) to neutral (pH 7), while the particle size increases when the neutral solution is altered to a more basic medium. Since a larger surface area is desired, a pH value of 7 was considered the optimal parameter value.

In addition, the aqueous extract of *Zingiber officinal* was used in the biosynthesis of silver nanoparticles, where the effect of the pH level was evaluated [145]. The pH of the reaction was adjusted by varying the volume of NaOH added to the solution from 1 to 5 mL; thereby,

Preprints (www.preprints.org) | NOT PEER-REVIEWED | Posted: 17 February 2021 doi:10.20944/preprints202102.0380.v1

achieving pH values of 6, 8, 10, 12 and 14, respectively. The XRD results for each pH displayed equivalent peaks located at 2θ = 38.2°, 44.4°, 64.6°, 77.5° and 81.5° which are indexed to the (100), (200), (220), (311) and (222), respectively (Figure 6a). On the other hand, the peak intensities increased almost linearly from pH 6 to pH 14. This reflected that as the solution became more basic, size and crystallinity of the Ag nanoparticles increased. The SEM images further analysed the compounds, which revealed that the nanostructures were predominantly clustered; however, as the pH increased, the formation of the silver nanoparticles were more pronounced. In summary, the study found that the silver nanoparticles can be tuned by altering the hydrothermal conditions and changing the pH values.

Moreover, the green synthesis of silver nanoparticles was successfully carried out through reduction with *Pistia stratiotes* extract [146]. The pH level of the initial mixture was adjusted from 4 to 10, with increments of 2, by the addition of either hydrochloric acid (HCl) or ammonium hydroxide (NH_4OH). The researchers observed a colour change in the solution from yellow to brown within 5-10 minutes, assuming the formation of silver nanocolloids; this was confirmed by the analysis of the UV-vis spectrum (Figure 6c). The surface plasmon resonance peaks for pH 4 and pH 6 were found to be situated at approximately 330 nm, while the SPR peaks for pH 8 and pH 10 were observed at around 420 nm. Therefore, the acidic medium demonstrated a blueshift, deeming the particles smaller than that in the basic medium. In addition to this, the concentration of the acidity or basicity of the solution had a clear effect on the intensity of the absorption bands as the synthesis process favoured a more neutral solution. The TEM images of the nanoparticles confirmed the UV-vis results as the average diameters were revealed to be 16.55 nm and 20.41 nm in an acidic and basic medium, respectively.

Furthermore, Al-Radadi (2019) produced research on the effect of pH levels on the biosynthesis of platinum nanoparticles through the use of *Phoenix dactylifera* as a reducing and stabilising agent. The pH values were varied to 1.5, 3.5, 5.5 and 7.5 through the addition either 0.1 M HCl or 0.1 M NaOH solution. According to the TEM images obtained, the pH of the medium had an adverse effect on the morphology of the nanoparticles. It was found that with an increase in alkalinity, the formation of the nanostructures had increased where bundles of platinum were of heterogeneous shape and sizes, ranging from 2.3 nm to 22 nm. On the other hand, the normal pH (5.5), of the original mixture of between the metallic salt solution and the aqueous *Phoenix dactylifera* extract, exhibited the production of smaller particles that possessed a greater sphericity. Thereafter, Al-Radadi (2019) stated that if smaller nanoparticles are desired, a higher value of pH is required for the efficient capping of the platinum nanomaterial.

Therefore, depending on the nanomaterial being synthesised, the pH level has proven to have an adverse effect on the size, morphology and crystallinity of the nanostructures, with a more neutral pH being favoured throughout the majority of the studies researched due to the smaller diameters of the particles; therefore, denoting a higher reactivity for their applications.

Preprints (www.preprints.org) | NOT PEER-REVIEWED | Posted: 17 February 2021 doi:10.20944/preprints202102.0380.v1

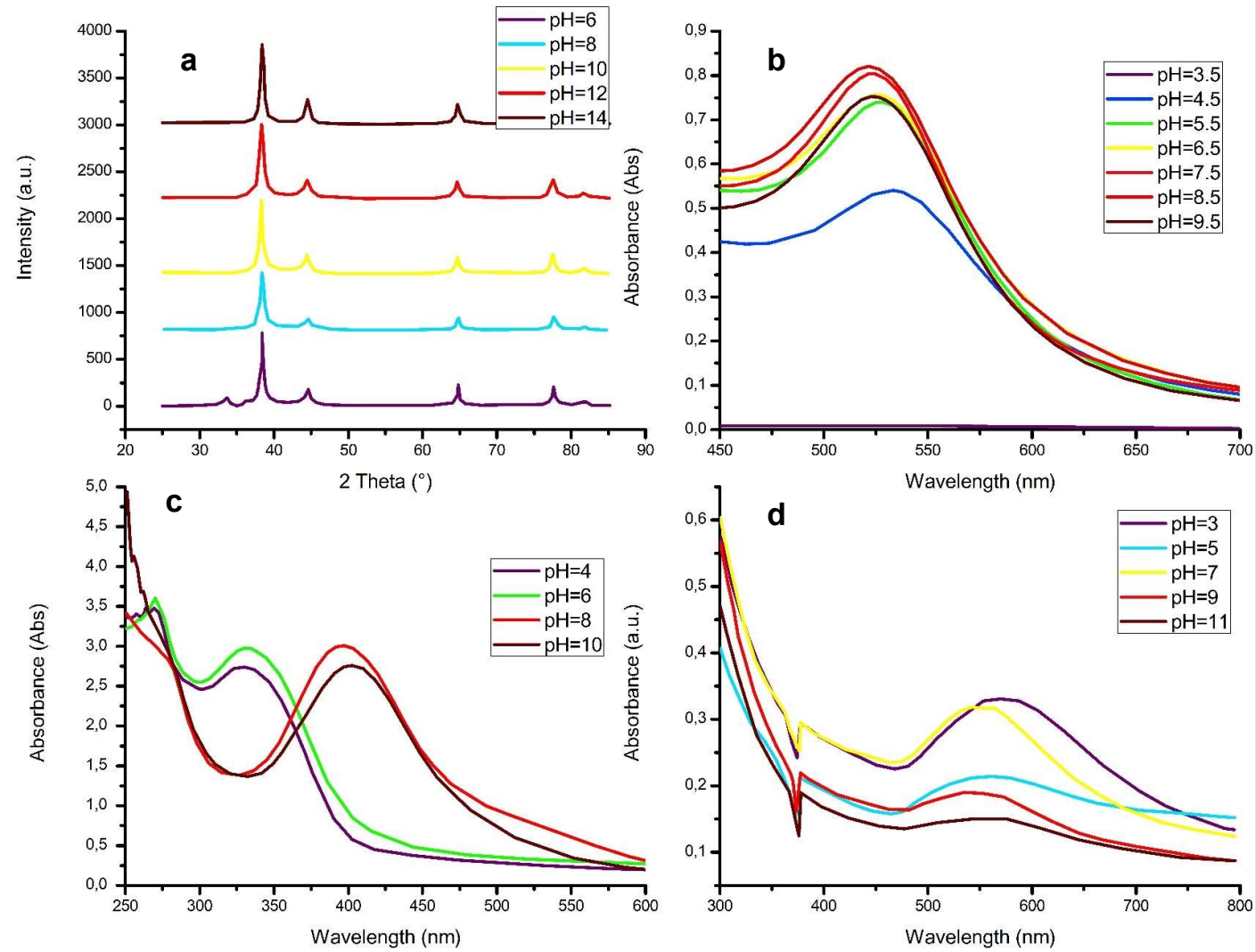

Figure 6: Readapted graphs of the, a) XRD pattern of AgNPs synthesised using Zingiber officinal under different pH conditions [145]*; b) UV-vis spectrum of the effect of initial pH on Elaeis guineensis-mediated AuNPs* [156]*; c) UV-vis spectra of AgNPs biosynthesised from Pistia stratiotes and how pH levels affect it* [146]*; d) UV-vis of Amomum subulatum-conjugated AuNPs at different pH values* [144].

Preprints (www.preprints.org) | NOT PEER-REVIEWED | Posted: 17 February 2021 doi:10.20944/preprints202102.0380.v1

4.5. Calcination Temperature

The calcination temperature of the process refers to the temperature at which the nanoparticles are stripped of their volatile substances. This procedure has been known to affect the characteristics of the nanostructures by refining their size, crystallinity and general stability of the nanomaterial.

In a study directed by Asemani & Anarjan (2019), copper oxide (CuO) nanoparticles were synthesised using *Juglans regia* leaf extract. The copper oxide nanomaterial was fabricated through the addition of the extract solution with copper nitrate, where the annealing temperature was altered to 300°C, 400°C and 500°C. The results of the experimentation displayed a correlation between the calcination temperature and the maximum wavelength and absorption of the solution. It was concluded that nanoparticles with smaller diameters were achieved through the use higher temperatures; in other words, 400-500°C.

Similarly, zinc oxide nanoparticles were fabricated with the use of *Anchusa italic* aqueous extract as a bioreducing and capping agent [148]. The effect of calcination temperature on the zinc oxide nanomaterial was then studied by varying the furnace temperature to 100°C and 200°C, where the samples were kept for 2 hours. The XRD analysis of the sample prepared at 100°C only displayed a few of the diffraction peaks for ZnO when compared to the nanoparticles calcined at 200°C (Figure 7b). Additionally, the peaks were considerably low in intensity, indicating low crystallinity. Azizi and co-authors (2016) stated that high temperatures are capable of providing sufficient kinetic energy to the process, thus, improving the crystal structure of the nanoparticles due to the reorder of the atomic arrangement. The average particle diameter of the nanostructures was calculated through the use of Scherrer's equation, which found particles sizes of approximately 10.8 nm and 16.2 nm for 100°C and 200°C, respectively. It was concluded that by increasing the annealing temperature, the crystal structure and the particle sizes were enhanced.

Furthermore, Mfon and co-authors (2020) demonstrated the effect of annealing temperature on *Ocimum gratissimum*-mediated zinc oxide nanoparticles. The study utilised two different calcination temperatures, namely, 250°C and 400°C for 3-hour time periods each. The SEM micrographs revealed that the nanomaterial synthesised at 400°C were spherical and had a wide range of colloids with clusters around larger particles. The nanostructures biosynthesised at 250°C also possessed spherical morphologies; on the other hand, the substance had a porous quality when compared to the latter. The crystalline size of the particles was calculated to be 29 nm and 14 nm for the calcination temperature of 400°C and 250°C, respectively. Therefore, Mfon and co-authors (2020) concluded that increasing the annealing temperature would, ultimately, increase the size of the nanoparticles.

Preprints (www.preprints.org) | NOT PEER-REVIEWED | Posted: 17 February 2021 doi:10.20944/preprints202102.0380.v1

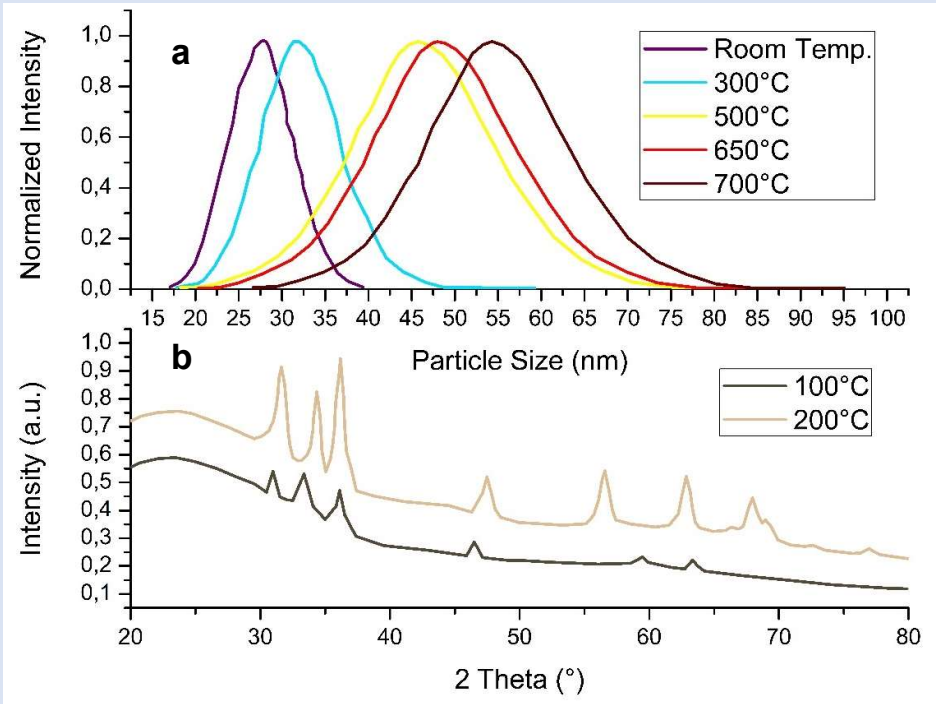

Figure 7: Readapted graphs of, a) UV-vis spectrum of ZnO NPs and the effect of annealing temperature on particle size [157]*; b) XRD analysis of biosynthesised ZnO nanoparticles using Anchusa italic extract* [148].

Preprints (www.preprints.org) | NOT PEER-REVIEWED | Posted: 17 February 2021 doi:10.20944/preprints202102.0380.v1

5. Conclusions and Future Perspective

In conclusion, the biosynthesis of transition-metal nanoparticles and their applications may be summarised accordingly:

- Plant extract-mediated nanoparticles have significant advantageous as they reduce the complexity of the procedure, inhibit the use of toxic chemicals and eliminate harmful by-products through the modification of chemical synthesise processes.
- All plants have a reductive capability, with species possessing different reducing strengths as a result of their major reductant. This has an effect on the concentration, size and morphology of the desired nanoparticles.
- Size and morphology give the nanoparticles their unique properties, however, controlling these characteristics precisely are still troublesome.
- Agglomeration is deemed as a major issue amongst nanoparticles as it may negatively affect their characteristics by reducing the available surface area.
- During synthesis, an increase in precursor concentration generally leads to an increase in particle diameter, concentration or agglomeration.
- An increase in synthesis temperature increases the reaction rate, thereby increasing the concentration of nanomaterial and narrowing the particle size range, assuming sufficient precursor.
- Increasing the reaction time subsequently increases concentration, size or agglomeration.
- The reaction solution generally favours a more neutral pH value, although increasing the pH level also increases the crystallinity of the material and may induce clusters to form.
- Particle diameter and crystallinity of the nanostructures increases with an increase in calcination temperature.

In addition, the characteristics of plant-mediated nanoparticles are still relatively unpredictable; however, the current knowledge on the subject and ongoing research is narrowing the space between known and unknown. Unfortunately, it is difficult to determine and control the properties of nanostructures by basing experimentation on the assumptions of previous research. Contrarily, a general trend may be utilised for further research in the field. Nevertheless, only macroscopic experimental observations were utilised to produce these conclusions, with no microscopic insight into mechanisms of the nanocolloids being taken into consideration.

Acknowledgments

The author acknowledges the financial support from the Cape Peninsula University of Technology (CPUT) Award.

Conflicts of Interest

On behalf of all authors, the corresponding author states that there is no conflict of interest

References

[1] S. Iravani, Green synthesis of metal nanoparticles using plants, Green Chem. 13 (2011) 2638–2650. https://doi.org/10.1039/c1gc15386b.

[2] K. Suvardhan, S. Ahmed, eds., Green Metal Nanoparticles: Synthesis, Characterisation and their Applications, Scrivener Publishing, 2013. https://doi.org/10.1017/CBO9781107415324.004.

[3] K. Sridharan, The Electromagnetic Spectrum, in: Spectr. Methods Transit. Met. Complexes, Elsevier, 2016: pp. 1–12. https://doi.org/10.1016/B978-0-12-809591-1.00001-3.

[4] A. Manchon, A. Belabbes, Spin-Orbitronics at Transition Metal Interfaces, Solid State Phys. 68 (2017) 1–89. https://doi.org/10.1016/BS.SSP.2017.07.001.

[5] A.-H. Ryaidh, M.A.J. Al-Qayim, Bio-Synthesis and Characterizations of Magnetic Iron Oxide Nanoparticles Mediated By Iraq Propolis Extract, IOSR J. Pharm. Biol. Sci. (IOSR-JPBS. 12 (2017) 65–73. https://doi.org/10.9790/3008-1206056573.

[6] A. Deljou, S. Goudarzi, Green extracellular synthesis of the silver nanoparticles using Thermophilic Bacillus Sp. AZ1 and its antimicrobial activity against several human pathogenetic bacteria, Iran. J. Biotechnol. 14 (2016) 25–32. https://doi.org/10.15171/ijb.1259.

[7] Z. Molnár, V. Bódai, G. Szakacs, B. Erdélyi, Z. Fogarassy, G. Sáfrán, T. Varga, Z. Kónya, E. Tóth-Szeles, R. Szucs, I. Lagzi, Green synthesis of gold nanoparticles by thermophilic filamentous fungi, Sci. Rep. 8 (2018) 1–12. https://doi.org/10.1038/s41598-018-22112-3.

[8] T. Kathiraven, A. Sundaramanickam, N. Shanmugam, T. Balasubramanian, Green synthesis of silver nanoparticles using marine algae Caulerpa racemosa and their antibacterial activity against some human pathogens, Appl. Nanosci. 5 (2015) 499–504. https://doi.org/10.1007/s13204-014-0341-2.

[9] F. Niknejad, M. Nabili, R. Daie Ghazvini, M. Moazeni, Green synthesis of silver nanoparticles: Another honor for the yeast model Saccharomyces cerevisiae, Curr. Med. Mycol. 1 (2015) 17–24. https://doi.org/10.18869/acadpub.cmm.1.3.17.

[10] H. Bar, D.K. Bhui, G.P. Sahoo, P. Sarkar, S.P. De, A. Misra, Green synthesis of silver nanoparticles using latex of Jatropha curcas, Colloids Surfaces A Physicochem. Eng. Asp. 339 (2009) 134–139. https://doi.org/10.1016/j.colsurfa.2009.02.008.

[11] J.L. Gardea-Torresdey, J.G. Parsons, E. Gomez, J. Peralta-Videa, H.E. Troiani, P. Santiago, M.J. Yacaman, Formation and Growth of Au Nanoparticles inside Live Alfalfa Plants, Nano Lett. 2 (2002) 397–401. https://doi.org/10.1021/nl015673+.

[12] M. Kowshik, S. Ashtaputre, S. Kharrazi, W. Vogel, J. Urban, S.K. Kulkarni, K.M. Paknikar, Extracellular synthesis of silver nanoparticles by a silver-tolerant yeast strain MKY3, Nanotechnology. 14 (2002) 95–100. https://doi.org/10.1088/0957-4484/14/1/321.

[13] H. Lee, A.M. Purdon, V. Chu, R.M. Westervelt, Controlled Assembly of Magnetic Nanoparticles from Magnetotactic Bacteria Using Microelectromagnets Arrays, Nano Lett. 4 (2004) 995–998. https://doi.org/10.1021/nl049562x.

[14] P. Mukherjee, S. Senapati, D. Mandal, A. Ahmad, M.I. Khan, R. Kumar, M. Sastry, Extracellular Synthesis of Gold Nanoparticles by the Fungus Fusarium oxysporum, ChemBioChem. 3 (2002) 461–463. https://doi.org/10.1002/1439-7633(20020503)3:5<461::AID-CBIC461>3.0.CO;2-X.

[15] X. Li, H. Xu, Z.-S. Chen, G. Chen, Biosynthesis of Nanoparticles by Microorganisms and Their Applications, J. Nanomater. 2011 (2011) 270974. https://doi.org/10.1155/2011/270974.

[16] P. Singh, Y.-J. Kim, D. Zhang, D.-C. Yang, Biological Synthesis of Nanoparticles from Plants and Microorganisms, Trends Biotechnol. 34 (2016) 588–599. https://doi.org/10.1016/J.TIBTECH.2016.02.006.

[17] I. Hussain, N.B. Singh, A. Singh, H. Singh, S.C. Singh, Green synthesis of nanoparticles and its potential application, Biotechnol. Lett. 38 (2016) 545–560. https://doi.org/10.1007/s10529-015-2026-7.

[18] O. V. Kharissova, H.V.R. Dias, B.I. Kharisov, B.O. Pérez, V.M.J. Pérez, The greener synthesis of nanoparticles, Trends Biotechnol. 31 (2013) 240–248. https://doi.org/10.1016/j.tibtech.2013.01.003.

[19] R.K. Das, V.L. Pachapur, L. Lonappan, M. Naghdi, R. Pulicharla, S. Maiti, M. Cledon, L.M.A. Dalila, S.J. Sarma, S.K. Brar, Biological synthesis of metallic nanoparticles: plants, animals and microbial aspects, Nanotechnol. Environ. Eng. 2 (2017) 18. https://doi.org/10.1007/s41204-017-0029-4.

[20] A. Rastogi, P. Singh, F.A. Haraz, Biological synthesis of nanoparticles: an environmentally benign approach, Fundam. Nanoparticles. (2018) 571–604. https://doi.org/10.1016/B978-0-323-51255-8.00023-9.

[21] M. Ovais, A.T. Khalil, N.U. Islam, I. Ahmad, M. Ayaz, M. Saravanan, Z.K. Shinwari, S. Mukherjee, Role of plant phytochemicals and microbial enzymes in biosynthesis of metallic nanoparticles, Appl. Microbiol. Biotechnol. 102 (2018) 6799–6814. https://doi.org/10.1007/s00253-018-9146-7.

[22] A. Böttger, U. Vothknecht, C. Bolle, A. Wolf, Lessons on caffeine, cannabis & Co., 2018. https://doi.org/10.1007/978-3-319-99546-5.

[23] A. Krishnasamy, M. Sundaresan, P. Velan, Rapid phytosynthesis of nano-sized titanium using leaf extract of Azadirachta indica, Int. J. ChemTech Res. 8 (2015) 2047–2052.

[24] S. Kalyanasundaram, M.J. Prakash, Biosynthesis and Characterization of Titanium Dioxide Nanoparticles Using Pithecellobium Dulce and Lagenaria Siceraria Aqueous Leaf Extract and Screening their Free Radical Scavenging and Antibacterial Properties, Int. Lett. Chem. Phys. Astron. 50 (2015) 80–95. https://doi.org/10.18052/www.scipress.com/ilcpa.50.80.

[25] R. Dobrucka, The biological synthesis of anatase titanium dioxide nanoparticles using Arnicae anthodium extract, Bulg. Chem. Commun. 49 (2017) 595–599. http://www.bcc.bas.bg/BCC_Volumes/Volume_49_Number_3_2017/BCC-49-3-2017-Dobrucka-595-599.pdf.

[26] K. Rao, C. Ashok, K. Rao, C. Chakra, V. Rajendar, SYNTHESIS OF TIO2 NANOPARTICLES FROM ORANGE FRUIT WASTE, 2 (2015) 82–90.

[27] A. Chatterjee, D. Nishanthini, N. Sandhiya, J. Abraham, Biosynthesis of titanium

dioxide nanoparticles using Vigna radiata, Asian J. Pharm. Clin. Res. 9 (2016) 85–88.

[28] S.J. Bao, C. Lei, M.W. Xu, C.J. Cai, D.Z. Jia, Environment-friendly biomimetic synthesis of TiO 2 nanomaterials for photocatalytic application, Nanotechnology. 23 (2012). https://doi.org/10.1088/0957-4484/23/20/205601.

[29] M. Srinivasan, M. Venkatesan, V. Arumugam, G. Natesan, N. Saravanan, S. Murugesan, S. Ramachandran, R. Ayyasamy, A. Pugazhendhi, Green synthesis and characterization of titanium dioxide nanoparticles (TiO 2 NPs) using Sesbania grandiflora and evaluation of toxicity in zebrafish embryos, Process Biochem. 80 (2019) 197–202. https://doi.org/10.1016/j.procbio.2019.02.010.

[30] A.A. Zahir, I.S. Chauhan, A. Bagavan, C. Kamaraj, G. Elango, J. Shankar, N. Arjaria, S.M. Roopan, A.A. Rahuman, N. Singh, Green synthesis of silver and titanium dioxide nanoparticles using Euphorbia prostrata extract shows shift from apoptosis to G<inf>0</inf>/G<inf>1</inf> arrest followed by necrotic cell death in Leishmania donovani, Antimicrob. Agents Chemother. 59 (2015) 4782–4799. https://doi.org/10.1128/AAC.00098-15.

[31] P. Sahaya, M. Kumar, A.P. Francis, T. Devasena, Biosynthesized and Chemically Synthesized Titania Nanoparticles: Comparative Analysis of Antibacterial Activity, J. Environ. Nanotechnol. 3 (2014) 73–81. https://doi.org/10.13074/jent.2014.09.143098.

[32] G. Hoag, J. Collins, J. Holcomb, J. Hoag, M. Nadagouda, R. Varma, Degradation of bromothymol blue by 'greener' nano-scale zero-valent iron synthesized using tea polyphenols, J. Mater. Chem. 19 (2009) 8671–8677. https://doi.org/10.1039/B909148C.

[33] N. Latha, M. Gowri, Bio Synthesis and Characterisation of Fe 3 o 4 Nanoparticles Using Caricaya Papaya Leaves Extract, Int. J. Sci. Res. 3 (2014) 1551–1556.

[34] P.L. Pravallika, G.K. Mohan, K.V. Rao, K. Shanker, Biosynthesis, characterization and acute oral toxicity studies of synthesized iron oxide nanoparticles using ethanolic extract of Centella asiatica plant, Mater. Lett. 236 (2019) 256–259. https://doi.org/10.1016/j.matlet.2018.10.037.

[35] T. Naseem, M.A. Farrukh, Antibacterial activity of green synthesis of iron nanoparticles using lawsonia inermis and gardenia jasminoides leaves extract, J. Chem. 2015 (2015). https://doi.org/10.1155/2015/912342.

[36] R. Yuvakkumar, J. Suresh, A.J. Nathanael, M. Sundrarajan, S.I. Hong, Rambutan (Nephelium lappaceum L.) peel extract assisted biomimetic synthesis of nickel oxide nanocrystals, Mater. Lett. 128 (2014) 170–174. https://doi.org/10.1016/j.matlet.2014.04.112.

[37] P. Salgado, K. Márquez, O. Rubilar, D. Contreras, G. Vidal, The effect of phenolic compounds on the green synthesis of iron nanoparticles (Fe x O y -NPs) with photocatalytic activity, Appl. Nanosci. 9 (2019) 371–385. https://doi.org/10.1007/s13204-018-0931-5.

[38] E. Murgueitio, A. Debut, J. Landivar, L. Cumbal, Synthesis of iron nanoparticles through extracts of native fruits of Ecuador, as capuli (Prunus serotina) and mortiño (Vaccinium floribundum), Biol. Med. 8 (2016) 8–10. https://doi.org/10.4172/0974-8369.1000282.

[39] M.G. Balamurugan, S. Mohanraj, S. Kodhaiyolii, V. Pugalenthi, Ocimum sanctum leaf extract mediated green synthesis of iron oxide nanoparticles: spectroscopic and microscopic studies, JCHPS Spec. Issue. 4 (2014) 201–204. www.jchps.com.

[40] S. Amutha, S. Sridhar, Green synthesis of magnetic iron oxide nanoparticle using

leaves of Glycosmis mauritiana and their antibacterial activity against human pathogens, J. Innov. Pharm. Biol. Sci. 5 (2015) 22–26.

[41] J.K. Sharma, P. Srivastava, G. Singh, M.S. Akhtar, S. Ameen, Green synthesis of Co3O4 nanoparticles and their applications in thermal decomposition of ammonium perchlorate and dye-sensitized solar cells, Mater. Sci. Eng. B Solid-State Mater. Adv. Technol. 193 (2015) 181–188. https://doi.org/10.1016/j.mseb.2014.12.012.

[42] L. Han, D.P. Yang, A. Liu, Leaf-templated synthesis of 3D hierarchical porous cobalt oxide nanostructure as direct electrochemical biosensing interface with enhanced electrocatalysis, Biosens. Bioelectron. 63 (2015) 145–152. https://doi.org/10.1016/j.bios.2014.07.031.

[43] K. Ahmed, Green synthesis of cobalt nanoparticles by using methanol extract of plant leaf as reducing agent, Pure Appl. Biol. 5 (2016) 453–457. https://doi.org/10.19045/bspab.2016.50058.

[44] E.U. Ikhuoria, S.O. Omorogbe, B.T. Sone, M. Maaza, Bioinspired shape controlled antiferromagnetic Co3O4 with prism like-anchored octahedron morphology: A facile green synthesis using Manihot esculenta Crantz extract, Sci. Technol. Mater. (2018). https://doi.org/10.1016/j.stmat.2018.02.003.

[45] O. Igwe, Biofabrication of cobalt Nanoparticles using leaf extract of Chromolaena odorata and their potential antibacterial application, Res. J. Chem. Sci. 8 (2018) 11–17. http://www.isca.in/rjcs/Archives/v8/i1/2.ISCA-RJCS-2017-083.php.

[46] F.U. Okwunodulu, H.O. Chukwuemeka-Okorie, F.C. Okorie, Biological Synthesis of Cobalt Nanoparticles from Mangifera indica Leaf Extract and Application by Detection of Manganese (II) Ions Present in Industrial Wastewater, Chem. Sci. Int. J. 27 (2019) 1–8. https://doi.org/10.9734/csji/2019/v27i130106.

[47] K. Nomura, P. Terwilliger, M. Saeed, N. Akram, S. Ali, R. Naqvi, M. Usman, M.A. Abbas, Green and eco-friendly synthesis of Co3O4 and Ag-Co3O4: Characterisation and photo-catalytic activity, 8 (2019) 382–390.

[48] N. Matinise, N. Mayedwa, X.G. Fuku, N. Mongwaketsi, M. Maaza, Green synthesis of cobalt (II, III) oxide nanoparticles using Moringa Oleifera natural extract as high electrochemical electrode for supercapacitors, AIP Conf. Proc. 1962 (2018). https://doi.org/10.1063/1.5035543.

[49] J. Iqbal, B.A. Abbasi, R. Batool, A.T. Khalil, S. Hameed, S. Kanwal, I. Ullah, T. Mahmood, Biogenic synthesis of green and cost effective cobalt oxide nanoparticles using Geranium wallichianum leaves extract and evaluation of in vitro antioxidant, antimicrobial, cytotoxic and enzyme inhibition properties, Mater. Res. Express. 6 (2019) 115407. https://doi.org/10.1088/2053-1591/ab4f04.

[50] I. Bibi, N. Nazar, M. Iqbal, S. Kamal, H. Nawaz, S. Nouren, Y. Safa, K. Jilani, M. Sultan, S. Ata, F. Rehman, M. Abbas, Green and eco-friendly synthesis of cobalt-oxide nanoparticle: Characterization and photo-catalytic activity, Adv. Powder Technol. 28 (2017) 2035–2043. https://doi.org/10.1016/j.apt.2017.05.008.

[51] A. Diallo, A.C. Beye, T.B. Doyle, E. Park, M. Maaza, Green synthesis of Co_3O_4 nanoparticles via *Aspalathus linearis* : Physical properties, Green Chem. Lett. Rev. 8 (2015) 30–36. https://doi.org/10.1080/17518253.2015.1082646.

[52] S. Sudhasree, A. Shakila Banu, P. Brindha, G.A. Kurian, Synthesis of nickel nanoparticles by chemical and green route and their comparison in respect to biological effect and toxicity, Toxicol. Environ. Chem. 96 (2014) 743–754. https://doi.org/10.1080/02772248.2014.923148.

[53] I. Bibi, S. Kamal, A. Ahmed, M. Iqbal, S. Nouren, K. Jilani, N. Nazar, M. Amir, A. Abbas, S. Ata, F. Majid, Nickel nanoparticle synthesis using Camellia Sinensis as reducing and capping agent: Growth mechanism and photo-catalytic activity evaluation, Int. J. Biol. Macromol. 103 (2017) 783–790. https://doi.org/10.1016/j.ijbiomac.2017.05.023.

[54] N.M. Juibari, A. Eslami, Synthesis of nickel oxide nanorods by Aloe vera leaf extract: Study of its electrochemical properties and catalytic effect on the thermal decomposition of ammonium perchlorate, J. Therm. Anal. Calorim. 136 (2019) 913–923. https://doi.org/10.1007/s10973-018-7640-x.

[55] N. Sulaiman, Y. Yulizar, Spectroscopic, structural, and morphology of nickel oxide nanoparticles prepared using Physalis angulata leaf extract, Mater. Sci. Forum. 917 MSF (2018) 167–171. https://doi.org/10.4028/www.scientific.net/MSF.917.167.

[56] Z. Sabouri, A. Akbari, H.A. Hosseini, M. Darroudi, Facile green synthesis of NiO nanoparticles and investigation of dye degradation and cytotoxicity effects, J. Mol. Struct. 1173 (2018) 931–936. https://doi.org/10.1016/j.molstruc.2018.07.063.

[57] C.J. Pandian, R. Palanivel, S. Dhananasekaran, Green synthesis of nickel nanoparticles using Ocimum sanctum and their application in dye and pollutant adsorption, Chinese J. Chem. Eng. 23 (2015) 1307–1315. https://doi.org/10.1016/j.cjche.2015.05.012.

[58] M.A. Nasseri, F. Ahrari, B. Zakerinasab, A green biosynthesis of NiO nanoparticles using aqueous extract of Tamarix serotina and their characterization and application, Appl. Organomet. Chem. 30 (2016) 978–984. https://doi.org/10.1002/aoc.3530.

[59] S.M. Helen, M.H.E. Rani, Characterization and Antimicrobial Study of Nickel Nanoparticles Synthesized from Dioscorea (Elephant Yam) by Green Route, Int. J. Sci. Res. 4 (2015) 216–219. https://doi.org/10.21275/v4i11.nov151105.

[60] J. Iqbal, B.A. Abbasi, T. Mahmood, S. Hameed, A. Munir, S. Kanwal, Green synthesis and characterizations of Nickel oxide nanoparticles using leaf extract of Rhamnus virgata and their potential biological applications, Appl. Organomet. Chem. 33 (2019) 1–16. https://doi.org/10.1002/aoc.4950.

[61] F.T. Thema, E. Manikandan, A. Gurib-Fakim, M. Maaza, Single phase Bunsenite NiO nanoparticles green synthesis by Agathosma betulina natural extract, J. Alloys Compd. 657 (2016) 655–661. https://doi.org/10.1016/j.jallcom.2015.09.227.

[62] H. Chen, J. Wang, D. Huang, X. Chen, J. Zhu, D. Sun, J. Huang, Q. Li, Plant-mediated synthesis of size-controllable Ni nanoparticles with alfalfa extract, Mater. Lett. 122 (2014) 166–169. https://doi.org/10.1016/j.matlet.2014.02.028.

[63] M. Nasrollahzadeh, S.M. Sajadi, M. Khalaj, Green synthesis of copper nanoparticles using aqueous extract of the leaves of Euphorbia esula L and their catalytic activity for ligand-free Ullmann-coupling reaction and reduction of 4-nitrophenol, RSC Adv. 4 (2014) 47313–47318. https://doi.org/10.1039/c4ra08863h.

[64] G. Caroling, E. Vinodhini, A.M. Ranjitham, P. Shanthi, Biosynthesis of Copper Nanoparticles Using Aqueous Phyllanthus embilica– Characterisation and Study of Antibacterial Effects, Int. J. Pharm. Biol. Sci. 5 (2015) 25–43.

[65] H. Veisi, S. Hemmati, H. Javaheri, N-Arylation of indole and aniline by a green synthesized CuO nanoparticles mediated by Thymbra spicata leaves extract as a recyclable and heterogeneous nanocatalyst, Tetrahedron Lett. 58 (2017) 3155–3159. https://doi.org/10.1016/j.tetlet.2017.06.086.

[66] M. Altikatoglu, A. Attar, F. Erci, C.M. Cristache, I. Isildak, Green synthesis of copper

oxide nanoparticles using ocimum basilicum extract and their antibacterial activity, Fresenius Environ. Bull. 25 (2017) 7832–7837.

[67] N. Jayarambabu, A. Akshaykranth, T. Venkatappa Rao, K. Venkateswara Rao, R. Rakesh Kumar, Green synthesis of Cu nanoparticles using Curcuma longa extract and their application in antimicrobial activity, Mater. Lett. 259 (2020) 126813. https://doi.org/10.1016/j.matlet.2019.126813.

[68] G. Sharmila, R. Sakthi Pradeep, K. Sandiya, S. Santhiya, C. Muthukumaran, J. Jeyanthi, N. Manoj Kumar, M. Thirumarimurugan, Biogenic synthesis of CuO nanoparticles using Bauhinia tomentosa leaves extract: Characterization and its antibacterial application, J. Mol. Struct. 1165 (2018) 288–292. https://doi.org/10.1016/j.molstruc.2018.04.011.

[69] M. Maham, S.M. Sajadi, M.M. Kharimkhani, M. Nasrollahzadeh, Biosynthesis of the CuO nanoparticles using Euphorbia Chamaesyce leaf extract and investigation of their catalytic activity for the reduction of 4-nitrophenol, IET Nanobiotechnology. 11 (2017) 766–772. https://doi.org/10.1049/iet-nbt.2016.0254.

[70] N. Nagar, V. Devra, Green synthesis and characterization of copper nanoparticles using Azadirachta indica leaves, Mater. Chem. Phys. 213 (2018) 44–51. https://doi.org/10.1016/j.matchemphys.2018.04.007.

[71] D. Pawar, S. Shaikh, D. Shulaksana, R. Kanawade, Green synthesis of copper nanoparticles using Gloriosa superba L leaf extract, Int. J. Pharm. Pharm. Res. (2017) 203–209.

[72] K.S. Prasad, A. Patra, G. Shruthi, S. Chandan, Aqueous extract of saraca indica leaves in the synthesis of copper oxide nanoparticles: Finding a way towards going green, J. Nanotechnol. 2017 (2017). https://doi.org/10.1155/2017/7502610.

[73] G. Sulaiman, A. Tawfeeq, M. Jaaffer, Biogenic synthesis of copper oxide nanoparticles using Olea europaea leaf extract and evaluation of their toxicity activities: An in vivo and in vitro study, Biotechnol. Prog. 34 (2017) DOI: 10.1002/btpr.2568. https://doi.org/10.1002/btpr.2568.

[74] A.M. Awwad, B.A. Albiss, N.M. Salem, Antibacterial Activity of synthesized Copper Oxide Nanoparticles using Malva sylvestris Leaf Extract, SMU Med. J. 2 (2015) 91–101.

[75] G. Sangeetha, S. Rajeshwari, R. Venckatesh, Green synthesis of zinc oxide nanoparticles by aloe barbadensis miller leaf extract: Structure and optical properties, Mater. Res. Bull. 46 (2011) 2560–2566. https://doi.org/10.1016/j.materresbull.2011.07.046.

[76] J. Qu, X. Yuan, X. Wang, P. Shao, Zinc accumulation and synthesis of ZnO nanoparticles using Physalis alkekengi L., Environ. Pollut. 159 (2011) 1783–1788. https://doi.org/10.1016/j.envpol.2011.04.016.

[77] S. Narendhran, R. Sivaraj, Biogenic ZnO nanoparticles synthesized using L. aculeata leaf extract and~ their antifungal activity against plant fungal pathogens, Bull. Mater. Sci. 39 (2016) 1–5. https://doi.org/10.1007/s12034-015-1136-0.

[78] S. Devasenan, N. Hajara Beevi, S.S. Jayanthi, Green synthesis and characterization of zinc nanoparticle using Andrographis paniculata leaf extract, Int. J. Pharm. Sci. Rev. Res. 39 (2016) 243–247.

[79] N. Paul, A. Syed, P. Vyawahare, R. Dakle, B. Ghuge, Green Approach for the Synthesis of Zinc Nanoparticles and Its Antibacterial Activity, Int. Res. J. Pharm. 7 (2016) 99–102. https://doi.org/10.7897/2230-8407.07673.

[80] M. Ramesh, M. Anbuvannan, G. Viruthagiri, Green synthesis of ZnO nanoparticles using Solanum nigrum leaf extract and their antibacterial activity, Spectrochim. Acta Part A Mol. Biomol. Spectrosc. 136 (2015) 864–870. https://doi.org/10.1016/J.SAA.2014.09.105.

[81] N. Paul, E. Khole, S. Jagtap, H. Tribhuvan, G. Kakde, Green Synthesis of Zinc Nanowires using Spilanthes acmella Leaf Extract, UK J. Pharm. Biosci. 4 (2016) 45–47.

[82] K. Loganathan, P.V. Kumar, A.J. Ahamed, Biosynthesis of ZnO Nanoparticles using Phyllanthus Emblica Seed Powder and its Structural and Optical Characterization Studies, 7 (2018) 1–4.

[83] A. Datta, C. Patra, H. Bharadwaj, S. Kaur, N. Dimri, R. Khajuria, Green Synthesis of Zinc Oxide Nanoparticles Using Parthenium hysterophorus Leaf Extract and Evaluation of their Antibacterial Properties, J. Biotechnol. Biomater. 07 (2017) 3–7. https://doi.org/10.4172/2155-952x.1000271.

[84] R. Devi, R. Gayathri, Green Synthesis of Zinc Oxide Nanoparticles by using Hibiscus rosa-sinensis, Int. J. Curr. Eng. Technol. 44 (2014) 2444–2446. http://inpressco.com/category/ijcet.

[85] R. Dobrucka, J. Długaszewska, Biosynthesis and antibacterial activity of ZnO nanoparticles using Trifolium pratense flower extract, Saudi J. Biol. Sci. 23 (2016) 517–523. https://doi.org/10.1016/j.sjbs.2015.05.016.

[86] T. Karnan, S.A.S. Selvakumar, Biosynthesis of ZnO nanoparticles using rambutan (Nephelium lappaceumL.) peel extract and their photocatalytic activity on methyl orange dye, Elsevier Ltd, 2016. https://doi.org/10.1016/j.molstruc.2016.07.029.

[87] K. Elumalai, S. Velmurugan, S. Ravi, V. Kathiravan, S. Ashokkumar, Facile, eco-friendly and template free photosynthesis of cauliflower like ZnO nanoparticles using leaf extract of Tamarindus indica (L.) and its biological evolution of antibacterial and antifungal activities, Spectrochim. Acta - Part A Mol. Biomol. Spectrosc. 136 (2015) 1052–1057. https://doi.org/10.1016/j.saa.2014.09.129.

[88] M. Sathishkumar, K. Sneha, I.S. Kwak, J. Mao, S.J. Tripathy, Y.S. Yun, Phyto-crystallization of palladium through reduction process using Cinnamom zeylanicum bark extract, J. Hazard. Mater. 171 (2009) 400–404. https://doi.org/10.1016/j.jhazmat.2009.06.014.

[89] T.V. Surendra, S.M. Roopan, M.V. Arasu, N.A. Al-Dhabi, G.M. Rayalu, RSM optimized Moringa oleifera peel extract for green synthesis of M. oleifera capped palladium nanoparticles with antibacterial and hemolytic property, J. Photochem. Photobiol. B Biol. 162 (2016) 550–557. https://doi.org/10.1016/j.jphotobiol.2016.07.032.

[90] G. Sharmila, M. Farzana Fathima, S. Haries, S. Geetha, N. Manoj Kumar, C. Muthukumaran, Green synthesis, characterization and antibacterial efficacy of palladium nanoparticles synthesized using Filicium decipiens leaf extract, J. Mol. Struct. 1138 (2017) 35–40. https://doi.org/10.1016/j.molstruc.2017.02.097.

[91] M. Rafi Shaik, Z.J.Q. Ali, M. Khan, M. Kuniyil, M.E. Assal, H.Z. Alkhathlan, A. Al-Warthan, M.R.H. Siddiqui, M. Khan, S.F. Adil, Green synthesis and characterization of palladium nanoparticles using origanum vulgare L. extract and their catalytic activity, Molecules. 22 (2017). https://doi.org/10.3390/molecules22010165.

[92] E. Ismail, M. Khenfouch, M. Dhlamini, S. Dube, M. Maaza, Green palladium and palladium oxide nanoparticles synthesized via Aspalathus linearis natural extract, J. Alloys Compd. 695 (2017) 3632–3638. https://doi.org/10.1016/j.jallcom.2016.11.390.

[93] P. Dauthal, M. Mukhopadhyay, Biosynthesis of palladium nanoparticles using delonix regia leaf extract and its catalytic activity for nitro-aromatics hydrogenation, Ind. Eng. Chem. Res. 52 (2013) 18131–18139. https://doi.org/10.1021/ie403410z.

[94] A. Kanchana, S. Devarajan, S.R. Ayyappan, Green synthesis and characterization of palladium nanoparticles and its conjugates from solanum trilobatum leaf extract, Nano-Micro Lett. 2 (2010) 169–176. https://doi.org/10.5101/nml.v2i3.p169-176.

[95] A. Attar, M. Altikatoglu Yapaoz, Biosynthesis of palladium nanoparticles using Diospyros kaki leaf extract and determination of antibacterial efficacy, Prep. Biochem. Biotechnol. 48 (2018) 629–634. https://doi.org/10.1080/10826068.2018.1479862.

[96] V. Manikandan, P. Velmurugan, J.H. Park, N. Lovanh, S.K. Seo, P. Jayanthi, Y.J. Park, M. Cho, B.T. Oh, Synthesis and antimicrobial activity of palladium nanoparticles from Prunus × yedoensis leaf extract, Mater. Lett. 185 (2016) 335–338. https://doi.org/10.1016/j.matlet.2016.08.120.

[97] V. Gopinath, D. MubarakAli, S. Priyadarshini, N.M. Priyadharsshini, N. Thajuddin, P. Velusamy, Biosynthesis of silver nanoparticles from Tribulus terrestris and its antimicrobial activity: A novel biological approach, Colloids Surfaces B Biointerfaces. 96 (2012) 69–74. https://doi.org/10.1016/j.colsurfb.2012.03.023.

[98] K. Rao Kudle, J. Alwala, M.R. Donda, A. Miryala, B. Sreedhar, M. Pratap Rudra, Synthesis of silver nanoparticles using extracts of Securinega leucopyrus and evaluation of its antibacterial activity Collaborative Book Project on Phytochemistry View project Green synthesis View project Synthesis of silver nanoparticles using extracts , (2013). www.currentsciencejournal.info.

[99] B. Kumar, K. Smita, L. Cumbal, A. Debut, Green synthesis of silver nanoparticles using Andean blackberry fruit extract, Saudi J. Biol. Sci. 24 (2017) 45–50. https://doi.org/10.1016/j.sjbs.2015.09.006.

[100] S. Arokiyaraj, S. Vincent, M. Saravanan, Y. Lee, Y.K. Oh, K.H. Kim, Green synthesis of silver nanoparticles using Rheum palmatum root extract and their antibacterial activity against Staphylococcus aureus and Pseudomonas aeruginosa, Artif. Cells, Nanomedicine Biotechnol. 45 (2017) 372–379. https://doi.org/10.3109/21691401.2016.1160403.

[101] B.N. Rashmi, S.F. Harlapur, B. Avinash, C.R. Ravikumar, H.P. Nagaswarupa, M.R. Anil Kumar, K. Gurushantha, M.S. Santosh, Facile green synthesis of silver oxide nanoparticles and their electrochemical, photocatalytic and biological studies, Inorg. Chem. Commun. 111 (2020) 107580. https://doi.org/10.1016/J.INOCHE.2019.107580.

[102] V. Manikandan, P. Velmurugan, J.-H. Park, W.-S. Chang, Y.-J. Park, J. Palaniyappan, M. Cho, B.-T. Oh, Green synthesis of silver oxide nanoparticles and its antibacterial activity against dental pathogens, 3 Biotech. 7 (2017). https://doi.org/10.1007/s13205-017-0670-4.

[103] S. Ravichandran, V. Paluri, G. Kumar, K. Loganathan, B.R. Kokati Venkata, A novel approach for the biosynthesis of silver oxide nanoparticles using aqueous leaf extract of Callistemon lanceolatus (Myrtaceae) and their therapeutic potential, J. Exp. Nanosci. 11 (2016) 445–458. https://doi.org/10.1080/17458080.2015.1077534.

[104] B. Sadeghi, F. Gholamhoseinpoor, A study on the stability and green synthesis of silver nanoparticles using Ziziphora tenuior (Zt) extract at room temperature, Spectrochim. Acta - Part A Mol. Biomol. Spectrosc. 134 (2015) 310–315. https://doi.org/10.1016/j.saa.2014.06.046.

[105] K. Saware, A. Venkataraman, Biosynthesis and Characterization of Stable Silver

Nanoparticles Using Ficus religiosa Leaf Extract: A Mechanism Perspective, J. Clust. Sci. 25 (2014) 1157–1171. https://doi.org/10.1007/s10876-014-0697-1.

[106] M. Idrees, S. Batool, T. Kalsoom, S. Raina, H.M.A. Sharif, S. Yasmeen, Biosynthesis of silver nanoparticles using Sida acuta extract for antimicrobial actions and corrosion inhibition potential, Environ. Technol. (United Kingdom). 40 (2019) 1071–1078. https://doi.org/10.1080/09593330.2018.1435738.

[107] I. Alghoraibia, C. Soukkarieh, R. Zein, A. Alahmad, J.-G. Walter, M. Daghestani, Aqueous extract of Eucalyptus Camaldulensis leaves as reducing and capping agent in green synthesis of silver nanoparticles, Curr. Nanomater. 04 (2019) 1–9. https://doi.org/10.2174/2405461504666190625121807.

[108] V. Goodarzi, H. Zamani, L. Bajuli, A. Moradshahi, Evaluation of antioxidant potential and reduction capacity of some plant extracts in silver nanoparticles' synthesis., Mol. Biol. Res. Commun. 3 (2014) 165–174. https://doi.org/10.22099/mbrc.2014.2196.

[109] R. Karthik, R. Sasikumar, S.M. Chen, M. Govindasamy, J. Vinoth Kumar, V. Muthuraj, Green synthesis of platinum nanoparticles using Quercus glauca extract and its electrochemical oxidation of hydrazine in water samples, Int. J. Electrochem. Sci. 11 (2016) 8245–8255. https://doi.org/10.20964/2016.10.62.

[110] P.V. Kumar, S.M. Jelastin Kala, K.S. Prakash, Green synthesis derived Pt-nanoparticles using Xanthium strumarium leaf extract and their biological studies, J. Environ. Chem. Eng. 7 (2019) 103146. https://doi.org/10.1016/j.jece.2019.103146.

[111] K. Tahir, S. Nazir, A. Ahmad, B. Li, A.U. Khan, Z.U.H. Khan, F.U. Khan, Q.U. Khan, A. Khan, A.U. Rahman, Facile and green synthesis of phytochemicals capped platinum nanoparticles and in vitro their superior antibacterial activity, J. Photochem. Photobiol. B Biol. 166 (2017) 246–251. https://doi.org/10.1016/j.jphotobiol.2016.12.016.

[112] S.U. Ganaie, T. Abbasi, S.A. Abbasi, Biomimetic synthesis of platinum nanoparticles utilizing a terrestrial weed Antigonon leptopus, Part. Sci. Technol. 36 (2018) 681–688. https://doi.org/10.1080/02726351.2017.1292336.

[113] R. Dobrucka, Synthesis and Structural Characteristic of Platinum Nanoparticles Using Herbal Bidens Tripartitus Extract, J. Inorg. Organomet. Polym. Mater. 26 (2016) 219–225. https://doi.org/10.1007/s10904-015-0305-3.

[114] L. Castro, M.L. Blázquez, F. González, J.Á. Muñoz, A. Ballester, Biosynthesis of silver and platinum nanoparticles using orange peel extract: Characterisation and applications, IET Nanobiotechnology. 9 (2015) 252–258. https://doi.org/10.1049/iet-nbt.2014.0063.

[115] U. Jeyapaul, M.J. Kala, A.J. Bosco, P. Piruthiviraj, M. Easuraja, An eco-friendly approach for synthesis of platinum nanoparticles using leaf extracts of jatropa gossypifolia and jatropa glandulifera and their antibacterial activity, Orient. J. Chem. 34 (2018) 783–790. https://doi.org/10.13005/ojc/340223.

[116] R. Dobrucka, Biofabrication of platinum nanoparticles using Fumariae herba extract and their catalytic properties, Saudi J. Biol. Sci. 26 (2019) 31–37. https://doi.org/10.1016/j.sjbs.2016.11.012.

[117] K.P. Kumar, W. Paul, C.P. Sharma, Green synthesis of gold nanoparticles with Zingiber officinale extract: Characterization and blood compatibility, Process Biochem. 46 (2011) 2007–2013. https://doi.org/10.1016/j.procbio.2011.07.011.

[118] V. Ganesh Kumar, S. Dinesh Gokavarapu, A. Rajeswari, T. Stalin Dhas, V. Karthick, Z. Kapadia, T. Shrestha, I.A. Barathy, A. Roy, S. Sinha, Facile green synthesis of gold nanoparticles using leaf extract of antidiabetic potent Cassia auriculata, Colloids

Surfaces B Biointerfaces. 87 (2011) 159–163. https://doi.org/10.1016/j.colsurfb.2011.05.016.

[119] S.P. Dubey, M. Lahtinen, H. Särkkä, M. Sillanpää, Bioprospective of Sorbus aucuparia leaf extract in development of silver and gold nanocolloids, Colloids Surfaces B Biointerfaces. 80 (2010) 26–33. https://doi.org/10.1016/j.colsurfb.2010.05.024.

[120] B. Paul, B. Bhuyan, D.D. Purkayastha, S. Vadivel, S.S. Dhar, One-pot green synthesis of gold nanoparticles and studies of their anticoagulative and photocatalytic activities, Mater. Lett. 185 (2016) 143–147. https://doi.org/10.1016/j.matlet.2016.08.121.

[121] B. Ankamwar, Biosynthesis of gold nanoparticles (Green-Gold) using leaf extract of Terminalia Catappa, E-Journal Chem. 7 (2010) 1334–1339. https://doi.org/10.1155/2010/745120.

[122] S.Y. Lee, S. Krishnamurthy, C.W. Cho, Y.S. Yun, Biosynthesis of Gold Nanoparticles Using Ocimum sanctum Extracts by Solvents with Different Polarity, ACS Sustain. Chem. Eng. 4 (2016) 2651–2659. https://doi.org/10.1021/acssuschemeng.6b00161.

[123] A.M. Elbagory, C.N. Cupido, M. Meyer, A.A. Hussein, Large scale screening of southern African plant extracts for the green synthesis of gold nanoparticles using microtitre-plate method, Molecules. 21 (2016). https://doi.org/10.3390/molecules21111498.

[124] M. Noruzi, D. Zare, K. Khoshnevisan, D. Davoodi, Rapid green synthesis of gold nanoparticles using Rosa hybrida petal extract at room temperature, Spectrochim. Acta - Part A Mol. Biomol. Spectrosc. 79 (2011) 1461–1465. https://doi.org/10.1016/j.saa.2011.05.001.

[125] P. Elia, R. Zach, S. Hazan, S. Kolusheva, Z. Porat, Y. Zeiri, Green synthesis of gold nanoparticles using plant extracts as reducing agents, Int. J. Nanomedicine. 9 (2014) 4007–4021.

[126] S.O. Dozie-Nwachukwu, G. Etuk-Udo, J.D. Obayemi, N. Anuku, O.S. Odusanya, K. Malatesta, C. Chi, W.O. Soboyejo, Biosynthesis of Gold Nanoparticles from *Nauclea latifolia* Leaves, Adv. Mater. Res. 1132 (2015) 36–50. https://doi.org/10.4028/www.scientific.net/amr.1132.36.

[127] J. Huang, Q. Li, D. Sun, Y. Lu, Y. Su, X. Yang, H. Wang, Y. Wang, W. Shao, N. He, J. Hong, C. Chen, Biosynthesis of silver and gold nanoparticles by novel sundried Cinnamomum camphora leaf, Nanotechnology. 18 (2007). https://doi.org/10.1088/0957-4484/18/10/105104.

[128] L.B. Anigol, J.S. Charantimath, P.M. Gurubasavaraj, Effect of Concentration and pH on the Size of Silver Nanoparticles Synthesized by Green Chemistry, Org. Med. Chem. 3 (2017) 1–5. https://doi.org/10.19080/OMCIJ.2017.03.555622.

[129] P. Pratheema, Anti- Inflammatory And Anti- Bacterial Activity of Titanium Nanoparticles Synthesized From Rhizomes of Alpinia Calcarata, Int. J. Res. Appl. Sci. Eng. Technol. 6 (2018) 2472–2477. https://doi.org/10.22214/ijraset.2018.3563.

[130] S. Chauhan, L.S.B. Upadhyay, Biosynthesis of iron oxide nanoparticles using plant derivatives of Lawsonia inermis (Henna) and its surface modification for biomedical application, Nanotechnol. Environ. Eng. 4 (2019). https://doi.org/10.1007/s41204-019-0055-5.

[131] R. Faghihi, K. Larijani, V. Abdossi, P. Moradi, Green synthesis of silver nanoparticles by grapefruit‘s peel and effect on superoxide dismutase enzyme activity and growth of

cucumber plants inoculated with rhizoctonia solani, Orient. J. Chem. 33 (2017) 2810–2820. https://doi.org/10.13005/ojc/330614.

[132] M. Asemani, N. Anarjan, Green synthesis of copper oxide nanoparticles using Juglans regia leaf extract and assessment of their physico-chemical and biological properties, Green Process Synth. 8 (2019) 557–567. https://doi.org/10.1515/gps-2019-0025.

[133] F.M. Mohammadi, N. Ghasemi, Influence of temperature and concentration on biosynthesis and characterization of zinc oxide nanoparticles using cherry extract, J. Nanostructure Chem. 8 (2018) 93–102. https://doi.org/10.1007/s40097-018-0257-6.

[134] M. Vanaja, S. Rajeshkumar, K. Paulkumar, G. Gnanajobitha, C. Malarkodi, G. Annadurai, Kinetic study on green synthesis of silver nanoparticles using Coleus aromaticus leaf extract, Pelagia Res. Libr. 4 (2013) 50–55.

[135] R. Kumar, G. Ghoshal, A. Jain, M. Goyal, Rapid Green Synthesis of Silver Nanoparticles (AgNPs) Using (Prunus persica) Plants extract: Exploring its Antimicrobial and Catalytic Activities, J. Nanomed. Nanotechnol. 08 (2017). https://doi.org/10.4172/2157-7439.1000452.

[136] O. Stavinskaya, I. Laguta, T. Fesenko, M. Krumova, Effect of temperature on green synthesis of silver nanoparticles using vitex agnus-castus extract, Chem. J. Mold. 14 (2019) 117–121. https://doi.org/10.19261/cjm.2019.636.

[137] M.S. Latif, F. Kormin, M.K. Mustafa, I.I. Mohamad, M. Khan, S. Abbas, M.I. Ghazali, N.S. Shafie, M.F.A. Bakar, S.F. Sabran, S.F.Z.M. Fuzi, Effect of temperature on the synthesis of Centella asiatica flavonoids extract-mediated gold nanoparticles: UV-visible spectra analyses, in: AIP Conf. Proc., 2018. https://doi.org/10.1063/1.5055473.

[138] H. Liu, H. Zhang, J. Wang, J. Wei, Effect of temperature on the size of biosynthesized silver nanoparticle: Deep insight into microscopic kinetics analysis, Arab. J. Chem. 13 (2017) 1011–1019. https://doi.org/10.1016/j.arabjc.2017.09.004.

[139] R. Jon, N. Martin, P.R. Dasari, A. Paul, V. Singh, Effect of Physical Parameters on Green Synthesis of Gold Nanoparticles using Zea Mays Extract, Int. J. Eng. Adv. Technol. 9 (2019) 870–873. https://doi.org/10.35940/ijeat.f8819.129219.

[140] N.S. Pesika, K.J. Stebe, P.C. Searson, Relationship between Absorbance Spectra and Particle Size Distributions for Quantum-Sized Nanocrystals, J. Phys. Chem. B. 107 (2003) 10412–10415. https://doi.org/10.1021/jp0303218.

[141] N.A. Ramli, J. Jai, N.M. Yusof, Green synthesis of silver nanoparticles using elaeis guineensis (Palm Leaves): An investigation on the effect of reaction time in reduction mechanism and particle size, Appl. Mech. Mater. 575 (2014) 36–40. https://doi.org/10.4028/www.scientific.net/AMM.575.36.

[142] M. Behravan, A. Hossein Panahi, A. Naghizadeh, M. Ziaee, R. Mahdavi, A. Mirzapour, Facile green synthesis of silver nanoparticles using Berberis vulgaris leaf and root aqueous extract and its antibacterial activity, Int. J. Biol. Macromol. 124 (2019) 148–154. https://doi.org/10.1016/j.ijbiomac.2018.11.101.

[143] H.M.M. Ibrahim, Green synthesis and characterization of silver nanoparticles using banana peel extract and their antimicrobial activity against representative microorganisms, J. Radiat. Res. Appl. Sci. 8 (2015) 265–275. https://doi.org/10.1016/j.jrras.2015.01.007.

[144] A.K. Singh, O.N. Srivastava, One-Step Green Synthesis of Gold Nanoparticles Using Black Cardamom and Effect of pH on Its Synthesis, Nanoscale Res. Lett. 10 (2015). https://doi.org/10.1186/s11671-015-1055-4.

[145] W.J. Aziz, H.A. Jassim, A novel study of pH influence on Ag nanoparticles size with

antibacterial and antifungal activity using green synthesis, World Sci. News. 97 (2018) 139–152. www.worldscientificnews.com.

[146] P. Traiwatcharanon, K. Timsorn, C. Wongchoosuk, Effect of pH on the Green Synthesis of Silver Nanoparticles through Reduction with *Pistiastratiotes L.* Extract, Adv. Mater. Res. 1131 (2015) 223–226. https://doi.org/10.4028/www.scientific.net/amr.1131.223.

[147] N.S. Al-Radadi, Green synthesis of platinum nanoparticles using Saudi's Dates extract and their usage on the cancer cell treatment, Arab. J. Chem. 12 (2019) 330–349. https://doi.org/10.1016/j.arabjc.2018.05.008.

[148] S. Azizi, R. Mohamad, A. Bahadoran, S. Bayat, R.A. Rahim, A. Ariff, W.Z. Saad, Effect of annealing temperature on antimicrobial and structural properties of bio-synthesized zinc oxide nanoparticles using flower extract of Anchusa italica, J. Photochem. Photobiol. B Biol. 161 (2016) 441–449. https://doi.org/10.1016/j.jphotobiol.2016.06.007.

[149] R.E. Mfon, S.R. Hall, A. Sarua, Effect of ocimum gratissimum plant leaf extract concentration and annealing temperature on the structure and optical properties of synthesized zinc oxide nanoparticles, 7 (2020) 1–13.

[150] K. R, G. G, J. A, G. M, Rapid Green Synthesis of Silver Nanoparticles (AgNPs) Using (Prunus persica) Plants extract: Exploring its Antimicrobial and Catalytic Activities, J. Nanomed. Nanotechnol. 08 (2017). https://doi.org/10.4172/2157-7439.1000452.

[151] S.S. Muniandy, S. Sasidharan, H.L. Lee, Green synthesis of Ag nanoparticles and their performance towards antimicrobial properties, Sains Malaysiana. 48 (2019) 851–860. https://doi.org/10.17576/jsm-2019-4804-17.

[152] M.N. Chen, C.F. Chan, S.L. Huang, Y.S. Lin, Green biosynthesis of gold nanoparticles using Chenopodium formosanum shell extract and analysis of the particles' antibacterial properties, J. Sci. Food Agric. 99 (2019) 3693–3702. https://doi.org/10.1002/jsfa.9600.

[153] B. Rao, R.C. Tang, Green synthesis of silver nanoparticles with antibacterial activities using aqueous Eriobotrya japonica leaf extract, Adv. Nat. Sci. Nanosci. Nanotechnol. 8 (2017). https://doi.org/10.1088/2043-6254/aa5983.

[154] T. Ahmad, M. Irfan, M.A. Bustam, S. Bhattacharjee, Effect of Reaction Time on Green Synthesis of Gold Nanoparticles by Using Aqueous Extract of Elaise Guineensis (Oil Palm Leaves), Procedia Eng. 148 (2016) 467–472. https://doi.org/10.1016/j.proeng.2016.06.465.

[155] M. Darroudi, M. Bin Ahmad, R. Zamiri, A.K. Zak, A.H. Abdullah, N.A. Ibrahim, Time-dependent effect in green synthesis of silver nanoparticles, Int. J. Nanomedicine. 6 (2011) 677–681. https://doi.org/10.2147/IJN.S17669.

[156] M. Irfan, T. Ahmad, M. Moniruzzaman, B. Abdullah, Effect of pH on ionic liquid mediated synthesis of gold nanoparticle using elaiseguineensis (palm oil) kernel extract, IOP Conf. Ser. Mater. Sci. Eng. 204 (2017). https://doi.org/10.1088/1757-899X/204/1/012002.

[157] Z.N. Kayani, F. Saleemi, I. Batool, Effect of calcination temperature on the properties of ZnO nanoparticles, Appl. Phys. A Mater. Sci. Process. 119 (2015) 713–720. https://doi.org/10.1007/s00339-015-9019-1.